Concrete Uniaxial Nonlocal Damage-Plasticity Model for Simulating Post-Peak Response of Reinforced Concrete Beam-Columns under Cyclic Loading

Maha Kenawy, A.M.ASCE[1]; Sashi Kunnath, F.ASCE[2]; Subodh Kolwankar, M.ASCE[3]; and Amit Kanvinde, M.ASCE[4]

Abstract: Rigorous predication of localized deformations in reinforced concrete (RC) structures under cyclic loading is critical from the standpoint of seismic performance assessment. Among the available predictive tools, the fiber-discretized frame model is an attractive option for RC components because it captures the spread of plasticity and the interaction between the bending moment and axial force in a structural member, and can be generalized to different cross-sections from uniaxial material-level calibrations. However, in the presence of constitutive softening, this type of model suffers from pathological sensitivity to the mesh size of the finite element simulation, leading to nonphysical member response. A nonlocal methodology is presented to address these issues for RC beam-columns subjected to a combination of axial and cyclic lateral loads. The methodology is based on a uniaxial nonlocal constitutive model that is formulated in the combined framework of the theory of plasticity and damage mechanics. The model captures the observed strength and stiffness degradation of the concrete material under uniaxial compressive and tensile loading in addition to tension-compression transition effects. The model incorporates a length scale parameter that enforces interactions between neighboring material points, thereby overcoming the mesh sensitivity associated with the presence of constitutive softening. The scope of this study includes (1) developing the uniaxial damage-plasticity formulation for a fiber-based frame model, (2) developing a nonlocal damage formulation and proposing a simplified implementation approach to reduce the associated computational cost, and (3) interrogating the effect of different model parameters and making recommendations for characterizing all the associated parameters for RC frame member simulations. The performance of the nonlocal model is thoroughly assessed, and its predictive capability is demonstrated against experimental test data of 24 RC beam-columns subjected quasi-statically to reversed loading cycles. The limitations of the nonlocal methodology are discussed, and future research directions are highlighted. **DOI: 10.1061/(ASCE)ST.1943-541X.0002592.**

Author keywords: Concrete softening; Fiber models; Nonlocal formulations; Damage-plasticity; Frame elements.

Introduction and Background

The prediction of extreme limit states in structures, including collapse, is a major objective of performance-based earthquake engineering. Reinforced concrete (RC) moment frames are common seismic force-resisting systems in which members are anticipated to undergo flexural yielding and exhibit significant inelastic deformations under earthquake loading. Rigorous assessment of the expected performance of these systems necessitates accurate prediction of localized failure mechanisms, namely, crushing of the concrete, and buckling and fracture of the steel reinforcing bars. At the structural member or component scale, these phenomena cause the deterioration of the strength and stiffness of the member and lead to a negative stiffness or post-peak branch in the load-displacement response and eventually to structural collapse. In the framework of numerical simulations, research has demonstrated that the post-peak response of structural components is one of the major factors affecting the collapse response of a structural system (Ibarra and Krawinkler 2005). This was acknowledged by recent building guideline documents (e.g., ATC 2009; PEER 2010) that place large emphasis on the accurate simulation-based quantification of system response and assessment of collapse. In light of these trends, the characterization of the post-peak response of structures under extreme loads has gained increased interest in recent years within the structural engineering research community.

In most practical applications, nonlinear simulations of structures employ frame or line element models with either concentrated or distributed plasticity formulations. While the former type possesses superior computational performance, it suffers from drawbacks such as the need to presuppose the location and size of the concentrated plasticity zones (i.e., plastic hinges) and the inability to model the interaction between the bending moment and axial force in the member (P-M interaction). In contrast, distributed plasticity elements have gained popularity because of their ability to capture the initiation and spread of damage anywhere along the structural member. The fiber-discretized (FD) model is a distributed plasticity element type in which the member cross section is divided into fibers, and the section response is determined by aggregating the uniaxial response of each fiber. Therefore,

[1]Graduate Research Assistant, Dept. of Civil and Environmental Engineering, Univ. of California, Davis, CA 95616 (corresponding author). ORCID: https://orcid.org/0000-0002-9722-091X. Email: mmkenawy@ucdavis.edu

[2]Professor, Dept. of Civil and Environmental Engineering, Univ. of California, Davis, CA 95616.

[3]Graduate Research Assistant, Dept. of Civil and Environmental Engineering, Univ. of California, Davis, CA 95616.

[4]Professor, Dept. of Civil and Environmental Engineering, Univ. of California, Davis, CA 95616.

Note. This manuscript was submitted on September 12, 2019; approved on October 2, 2019; published online on February 20, 2020. Discussion period open until July 20, 2020; separate discussions must be submitted for individual papers. This paper is part of the ***Journal of Structural Engineering***, © ASCE, ISSN 0733-9445.

FD models are able to generalize cross sectional response from uniaxial material-level response and effectively capture P-M interaction in structural members using uniaxial constitutive models assigned to individual fibers. The performance of FD models is, however, compromised in the presence of a constitutive strain-softening behavior. It is well-established in the context of finite element (FE) simulations (Bažant and Belytschko 1985; Bažant and Lin 1988; Bažant and Jirásek 2002) that the boundary value problem loses ellipticity in the presence of strain-softening. As a result, the following problems can be identified in FD frame simulations of structural members with constitutive softening:

- Nonobjectivity of the member response with respect to the FE mesh size, meaning that the simulated load-deformation response of the member varies for different mesh sizes.
- Mesh-dependent localization of the inelastic deformations in the structural member, such that the localization zone (or plastic hinge) tends to a zero measure as the mesh is refined.

Coleman and Spacone (2001) studied the mesh sensitivity in FD frame element models and suggested an energy-based approach (Bažant and Oh 1983) to address the ensuing numerical problems and achieve an objective global member response. In more recent years, the nonlocal continuum theory was adopted in frame element models in various forms (Addessi and Ciampi 2007; Valipour and Foster 2009; Feng et al. 2015) to eliminate the softening-induced mesh sensitivity in the local and global response of structural members. The premise of the nonlocal constitutive theory, which emerged in continuum FE models in the 1960s, is to consider interactions between neighboring material locations within a certain characteristic length scale of the material. Consequently, the response (e.g., stress) at a location is assumed to be dependent on the deformation at that location and on the deformation profile in the vicinity of that location. In general, this approach has proved effective in eliminating the softening-induced mesh sensitivity and enforcing a mesh-independent strain localization zone (Bažant and Pijaudier-Cabot 1989; Jirásek and Zimmermann 1998; Brinkgreve 1994).

In frame element models, two different nonlocal approaches have emerged in recent years to overcome the mesh sensitivity of the softening response; the first of these approaches relies on introducing new element formulations that incorporate spatial gradients of deformation variables. An example of this approach is the gradient inelastic beam theory by Salehi and Sideris (2017) and Salehi and Sideris (2018). This theory decouples the nonlocality from the constitutive relations; therefore, it does not impose any restrictions on the form of the constitutive models. While shown to be effective, this type of model is limited to the force-based element model where the entire structural member is modeled as a single element; in other words, it does not permit nonlocal interactions between neighboring elements. Therefore, it appears not to be suited for the standard displacement-based frame FEs where multiple elements are typically required to model structural members.

The second approach to overcoming the softening-induced mesh sensitivity in frame models introduces nonlocal integral or gradient terms of state variables into the constitutive formulations. This approach has been implemented within three-dimensional continuum FE models in different constitutive frameworks, including models based on the theory of plasticity, damage mechanics, or a combination of both. Notable examples of the latter category include the nonlocal damage-plasticity formulations by Grassl and Jirásek (2006) and Xenos and Grassl (2016). Such models, however, have generally not been leveraged in seismic performance assessment applications due to their relative algorithmic complexity. In structural analysis applications with formulations based on the beam theory, the softening-induced localization appears at the level of the cross sectional deformations. Therefore, extending the nonlocal constitutive approach to beam elements should be focused on obtaining an objective cross sectional response (i.e., axial deformation and curvature). An example of such an approach was introduced into resultant plasticity frame elements in formulations such as Addessi and Ciampi (2007) and Zhang and Khandelwal (2016). In the context of the more attractive FD frame models, only a few studies (Valipour and Foster 2009; Kenawy et al. 2018; Feng et al. 2015) have proposed nonlocal approaches. Valipour and Foster (2009), for example, developed an integral nonlocal formulation with a damage model for concrete in a force-based element employing a secant stiffness approach. This formulation models concrete softening using a nonlocal damage parameter but does not include plastic deformations. More recently, an integral nonlocal formulation was developed by the authors (Kenawy et al. 2018) for a displacement-based element in which a nonlocal plastic strain variable was used to control the softening of concrete in a plasticity-based framework. This model approximated the uniaxial behavior of concrete as bilinear under compressive loading and disregarded the initial hardening behavior, stiffness degradation, and the behavior under tensile loading. Both of the preceding studies addressed localization in the sectional deformations indirectly by regularizing the stress-strain response of individual section fibers; an approach that seems to obtain reasonably good agreement with experimental tests. However, both studies addressed the issue in RC members subjected to monotonically increasing displacements only.

The extension of the fiber-based nonlocal constitutive approach to simulate the behavior of RC members subjected to cyclic loading poses several challenges. First, such a model should describe key features of the behavior of concrete under uniaxial cyclic loading, including plastic deformations, and strength and stiffness degradation under compressive and tensile loading. Second, the model should retain the relative algorithmic simplicity and ease of calibration that is characteristic of uniaxial material models and necessary from the standpoint of seismic performance assessment. Finally, and perhaps most importantly, the model must incorporate internal variables that increase monotonically to drive the progression of softening (e.g., cumulative plastic strain or damage parameters). This constitutive requirement has been well-studied (Jirásek 1998; Bažant and Jirásek 2002) and deemed necessary to achieve stability of the numerical solution. In fact, replacing the entire deformation field (total strain) with its nonlocal counterpart was shown to lead to zero-energy deformation modes in the FE solution (Bažant and Pijaudier-Cabot 1988). Accordingly, most studies in the literature select the nonlocal variables to be the field variables controlling the evolution of softening, and assume that the elastic behavior remains local. Another important consequence to this requirement is the difficulty of combining common uniaxial concrete models (e.g., Mander et al. 1988; Chang and Mander 1994; Yassin 1994; Martínez-Rueda and Elnashai 1997) with nonlocal concepts because these models rely on explicit relationships between the stress and total strain; i.e., no separate field variables exist for directly controlling the evolution of softening. As a result, very few studies to date have considered the development of a nonlocal constitutive approach to address the softening-induced issues in FD models of RC members subjected to cyclic or seismic loading. The work presented herein addresses this gap by proposing a nonlocal model for simulating the behavior of concrete under uniaxial cyclic loading in a mesh-independent manner within a fiber-based framework.

Scope and Contributions

The major contribution of the proposed framework is to enable the prediction of RC component deterioration under cyclic lateral

loading conditions in a rigorous and mesh-objective manner using a FD displacement-based frame element. The proposed model overcomes the deficiencies associated with modeling of concrete using FD frame elements and rule-based constitutive models which cannot capture softening because of their susceptibility to mesh sensitivity issues. The study consists of the following components: (1) developing a uniaxial damage-plasticity formulation that captures the observed permanent deformations and strength and stiffness degradation of concrete under compressive and tensile stress states; (2) developing and implementing a nonlocal damage formulation that incorporates spatial averages of the damage field variables within a certain length scale; (3) calibrating and providing recommendations for the model parameters, including the parameters controlling the stiffness degradation, the tension-compression transition behavior, and the associated nonlocal length scale; and (4) investigating the performance of the proposed model and validating its predictive capability against benchmark experimental data.

The proposed model extends the capability of a previously developed nonlocal displacement-based element framework (Kenawy et al. 2018) to cyclic and seismic loading applications. The model leverages salient aspects of the previously developed methodology while introducing important new features. The previously developed aspects include computing integral spatial averages of the deformation variables at the element level and using these averages to inform the softening evolution at the material level. In the earlier study by the authors, a bilinear plasticity model with a nonlocal softening variable was adopted to crudely represent the behavior of the concrete material under monotonic loading. In this work, a more sophisticated nonlocal constitutive model is proposed for use in both static and dynamic loading applications. The proposed model includes the following important features:

- In addition to accumulating plastic deformations under compressive stresses, the concrete material also exhibits hardening behavior prior to reaching the peak compressive strength, allowing for a more realistic representation of the initial stiffness and stiffness degradation of concrete prior to the peak. The material is also assumed to accumulate plastic deformations under tensile stresses. These features are accommodated by a local hardening plasticity model. The yield function of the model is assumed to have different yield values for uniaxial tensile and compressive stresses but is not appropriate for multiaxial loading.
- The softening behavior of the concrete under compressive and tensile stresses is represented by a damage mechanics-based model instead of the nonlocal plasticity approach adopted in the preceding work (Kenawy et al. 2018). The damage model controls both the strength degradation and the stiffness degradation observed during unloading and reloading. The model incorporates separate damage history variables under tension and compression, whose rates are related to the plastic strain rate. This is in contrast to the previous model that did not account for any stiffness degradation and therefore proved deficient in simulating the cyclic behavior of RC components where the stiffness degradation significantly affects the predicted response.
- The damage model is formulated such that the stiffness degradation is controlled by a single parameter, a secondary plastic modulus, under compression and under tension. This approach enables straightforward calibration of the model based on the observed stiffness degradation trends in uniaxial experimental tests. The direct calibration advantage comes as a result of developing and tailoring the model specifically for uniaxial loading, as opposed to the more involved calibration requirements of models developed for multiaxial loading applications (e.g., Grassl and Jirásek 2006).
- A novel plasticity-based approach is proposed for simulating the crack-closing behavior observed in concrete specimens during stress reversal from tension to compression (Ramtani et al. 1992). The approach relies upon a crack-closing modulus that determines the rate of closing of the tensile cracks under compressive stress. The proposed crack-closing feature further refines the ability of the model to capture the hysteresis loops that result from cyclic loading of RC components and introduces a new approach to simulating the cracking behavior of concrete that may be extended to other models.
- The damage model incorporates weighted spatial averages of the tension and compression damage history variables to enforce nonlocal interactions between neighboring material locations in the model within the associated length scale. The nonlocal character of the damage model eliminates the softening-induced mesh sensitivity issues. A simplified approach for evaluating the nonlocal damage history variables is presented to facilitate the numerical implementation of the nonlocal averaging procedure in modern object-oriented FE codes. This approach relies upon making simplifying approximations of the elastic strain distribution within the nonlocal averaging domain.

This paper is organized as follows: the following section presents the equations of the constitutive model, starting with the plasticity, local damage and crack-closing models, and followed by the nonlocal form of the damage formulation. Next, a discussion of the model parameters is presented, and recommendations are made for evaluating all parameters for RC simulations. Then, a schematic description of the numerical implementation of the entire nonlocal framework (which includes the nonlocal FD displacement-based frame element and the nonlocal constitutive model) is presented, followed by a discussion of the algorithmic implementation of the constitutive model. This discussion is followed by a description of several numerical studies that were conducted to assess the performance of the proposed nonlocal methodology in quasi-static RC structural simulations.

Nonlocal Concrete Constitutive Model

Constitutive Framework

The proposed damage-plasticity formulation describes the behavior of concrete under uniaxial cyclic loading. The plasticity part of the model is formulated in the effective stress space, where the effective stress $\bar{\sigma}$ represents the stress carried by an uncracked representative volume of the material for a given strain and is defined using the effective stress-strain law

$$\bar{\sigma} = E(\varepsilon - \varepsilon^p) \tag{1}$$

where ε and ε^p = total and plastic uniaxial strains, respectively; and E = elastic modulus. The nominal uniaxial stress σ, which represents the macro-level stress, is expressed as

$$\sigma = (1 - D)E(\varepsilon - \varepsilon^p) \tag{2}$$

where D = damage parameter which can take on values between 0 (undamaged state) to 1 (fully damaged state). The plasticity part of the model is independent of the damage part and is described by a yield function, flow rule, and loading-unloading conditions, respectively

$$f = f(\bar{\sigma}, k_c, k_t) \tag{3}$$

$$\dot{\varepsilon}^p = \dot{\lambda}\frac{\partial f}{\partial \bar{\sigma}} \tag{4}$$

$$f \le 0,\ \dot{\lambda} \ge 0,\ \dot{\lambda} f = 0 \tag{5}$$

where k_c = internal variable (or accumulated compressive plastic strain) that controls the evolution of the yield point in the one-dimensional model under compressive stress; and k_t = its counterpart under tensile stress. The over-dot denotes the material time rate, and $\dot{\lambda}$ = rate of the plastic multiplier.

The damage evolution under compression and tension is driven by damage history variables k_{dc} and k_{dt}, respectively. Under compressive stress, k_{dc} remains zero during the initial hardening of the material until the compressive strength f_c is reached. Beyond this limit, the damage variable starts growing such that its rate is controlled by the plastic strain rate. Under tensile stress, the material is assumed to not exhibit hardening behavior prior to softening. Therefore, the damage history variable k_{dt} starts growing simultaneously with the plasticity evolution after the material reaches the peak tensile stress f_t. Two separate damage parameters D_c and D_t are proposed to describe the material damage under compressive and tensile stress, respectively. The compression and tension damage parameters increase monotonically from 0 to 1 and are functions of the compression and tension damage history variables, respectively

$$D_c = g(k_{dc}) \tag{6}$$

$$D_t = g(k_{dt}) \tag{7}$$

Finally, the damage parameter D is a function of both D_c and D_t. The particular form of the yield and damage functions and the evolution of all history variables are described in the following subsections.

Plasticity Model

The yield function is assumed to take the following form:

$$f = |\bar{\sigma}| - \sigma_{yc}(k_c) + \alpha(\sigma_{yc}(k_c) - \sigma_{yt}(k_t)) \tag{8}$$

where $\sigma_{yc}(k_c)$ = yield stress under compression; $\sigma_{yt}(k_t)$ = yield stress under tension; and the parameter α is defined as follows:

$$\alpha = \begin{cases} 0.0 & \text{if } \bar{\sigma} \le 0.0 \\ 1.0 & \text{if } \bar{\sigma} > 0.0 \end{cases} \tag{9}$$

σ_{yc} is defined in the present model as follows:

$$\sigma_{yc}(k_c) = \begin{cases} f_y + Hk_c & k_c \le k_0 \\ f_c + H_d(k_c - k_0) & k_c > k_0 \end{cases} \tag{10}$$

where f_y = stress limit for the linear elastic response under compression; k_0 = value of the internal variable k_c at the peak compressive stress f_c. H and H_d = plastic moduli that must be positive; i.e., no softening is allowed in the plasticity model. The two parts of Eq. (10) describe the hardening of the material in the effective stress space for two different phases of the model. The first part of Eq. (10) represents a linear hardening response beyond the initial yield stress f_y and until the peak compressive stress f_c is reached. This particular linear function is used only to keep the model presentation and algorithmic implementation simple; however, it may be replaced by any form of nonlinear hardening. The second part of Eq. (10) describes the evolution of hardening beyond the peak stress and marks the beginning of the damage evolution, which is described by the damage model. The tensile yield stress σ_{yt} is defined as

$$\sigma_{yt}(k_t) = f_t + H_t k_t \tag{11}$$

where H_t = plastic modulus for the tensile behavior during damage evolution. The evolution laws for the compressive and tensile history variables are, respectively

$$\dot{k}_c = (1 - \alpha)|\dot{\varepsilon}^p| \tag{12}$$

$$\dot{k}_t = \alpha|\dot{\varepsilon}^p| \tag{13}$$

Damage Model

The damage part of the model controls both the strength and stiffness degradation of the material in the post-peak region under compressive and tensile stresses, and is enhanced with nonlocal history variables. The local form of the model is described in this subsection, whereas the nonlocal regularization is described later. The following proposed aspects enable straightforward calibration of the damage model:

- The strain-softening relationship under compression and tension is defined as an explicit relationship between the nominal stress and the inelastic strain (Grassl 2009), which is distinct from the plastic strain in this framework and defined later in Eq. (16).
- The hardening regime of the material under compression is separated into two phases (before and during the evolution of damage) with two different plastic moduli H and H_d to facilitate the calibration of both the hardening and softening parts of the model. This aspect is described mathematically in Eq. (10).
- The plastic moduli during the damage evolution under compression H_d and under tension H_t are treated as model parameters that solely control the evolution of the stiffness degradation in the model (i.e., the unloading stiffness during strain reversal) and are therefore directly calibrated to experimental observations. This calibration is performed in a subsequent section.

To separate the evolution of damage under compression and under tension, the damage parameter D is defined as follows:

$$D = (1 - \alpha)D_c + \alpha D_t \tag{14}$$

Therefore, the damage reduces to D_c under compressive stress states and D_t under tensile stress states. The particular forms of the compression and tension damage functions are developed in the following subsections.

Compression Damage Model

To define the strain-softening relationship under compressive stress, we note that $\alpha = 0.0$ under compressive stress and rewrite Eq. (2) as

$$\sigma = E(\varepsilon - (\varepsilon^p + D_c(\varepsilon - \varepsilon^p))) \tag{15}$$

where D reduces to D_c. Eq. (15) leads to the definition of the inelastic strain ε_i in the present framework as the term subtracted from the total strain

$$\varepsilon_i = \varepsilon^p + D_c(\varepsilon - \varepsilon^p) \tag{16}$$

The strain-softening form is assumed to take a modified form of the relationship proposed by Grassl (2009)

$$|\sigma| = f_c\left(1 - \frac{|\varepsilon_i| - k_0}{\varepsilon_f - k_0}\right) \tag{17}$$

This form defines a linear softening relationship between the magnitude of the nominal stress and the magnitude of the inelastic strain, such that the damage starts at $|\sigma| = f_c$ (i.e., the peak state) and increases linearly until it reaches the fully damaged state $\sigma = 0$

at the final total strain ε_f. The compression damage history variable k_{dc} is defined as

$$k_{dc} = k_c - k_0 \tag{18}$$

which represents the magnitude of the plastic strain beyond its value at the peak state. This definition leads to the following evolution equation for k_{dc}

$$\dot{k}_{dc} = \dot{k}_c \quad \text{if } k_c > k_0 \tag{19}$$

It is noted that the accumulation of damage occurs only during plastic loading beyond the peak state and cannot occur during unloading. Making use of this fact and Eqs. (12), (16), and (18), the magnitude of the inelastic strain during damage evolution may be rewritten as

$$|\varepsilon_i| = k_{dc} + k_0 + D_c|\varepsilon - \varepsilon^p|_{max} \tag{20}$$

where $|\varepsilon - \varepsilon^p|_{max}$ = value of the elastic strain during plastic loading. Similarly, during plastic loading, Eqs. (1) and (2) may be rewritten as follows:

$$|\bar{\sigma}| = E|\varepsilon - \varepsilon^p|_{max} \tag{21}$$

$$|\sigma| = (1 - D_c)E|\varepsilon - \varepsilon^p|_{max} \tag{22}$$

Noting the fact that $f = 0$ during plastic loading and substituting the second part of Eq. (10) and the definition of the damage history variable in Eq. (18) into Eq. (21), the value of the elastic strain during plastic loading beyond the peak state (i.e., during accumulation of damage) may be expressed as

$$|\varepsilon - \varepsilon^p|_{max} = \frac{\sigma_{yc}(k_c)}{E} = \frac{f_c + H_d(k_c - k_0)}{E} = \frac{f_c + H_d k_{dc}}{E} \tag{23}$$

where $|\varepsilon - \varepsilon^p|_{max}$ is expressed as a function of the damage history variable k_{dc} and material constants. Substituting Eqs. (20), (22), and (23) into Eq. (17) leads to the following form of the damage function in terms of the damage variable k_{dc}:

$$D_c(k_{dc}) = \frac{Ek_{dc}(H_d(\varepsilon_f - k_0) + f_c)}{(f_c + H_d k_{dc})(E(\varepsilon_f - k_0) - f_c)} \tag{24}$$

Eqs. (19) and (24) constitute the damage part of the model under compressive states. Eq. (19) determines the evolution of the compression damage history variable k_{dc}, whereas Eq. (24) explicitly determines the value of the damage parameter D_c as a function of k_{dc}.

Tension Damage Model

The post-peak response under tensile stress is described by a tension damage function that is derived in a manner similar to the compression damage function in Eq. (24). The key difference is that the evolution of damage coincides with the evolution of plasticity (i.e., no hardening is allowed in the model). Accordingly, the rate of the tension damage history variable k_{dt} is set equal to the rate of the internal variable k_t

$$\dot{k}_{dt} = \dot{k}_t \tag{25}$$

which leads to the following form of the tension damage function:

$$D_t(k_{dt}) = \frac{Ek_{dt}(H_t\varepsilon_{ft} + f_t)}{(f_t + H_t k_{dt})(E\varepsilon_{ft} - f_t)} \tag{26}$$

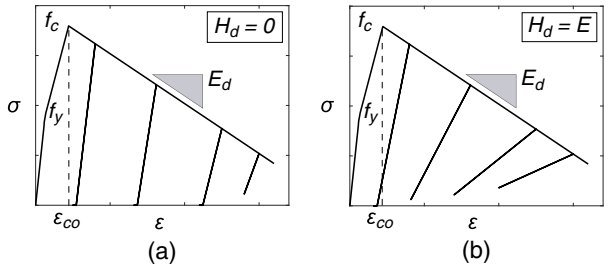

Fig. 1. Effect of the secondary plastic modulus H_d on the stiffness degradation of the constitutive model: (a) $H_d = 0$; and (b) $H_d = E$.

which is analogous to Eq. (24), and in which, the parameter ε_{ft} represents the strain at zero tensile stress (when no tensile capacity remains).

Unloading Stiffness

In the proposed damage functions in Eqs. (24) and (26), the damage is a function of the appropriate history variable, in addition to several material constants. Among these constants are the secondary plastic modulus H_d in compression, and the plastic modulus H_t in tension. These two constants do not influence the monotonic response of the model. Therefore, they cannot be calibrated from monotonic stress-strain relationships. These moduli, however, control the decomposition of the strain into elastic and plastic components. Therefore, they directly affect the unloading stiffness of the material. This effect is shown in Fig. 1 for different values of the modulus H_d in the compressive loading range. In the proposed framework, the moduli H_d and H_t are treated as model parameters that control the rate of stiffness degradation. These parameters are calibrated based on experimental observations of the stiffness degradation trends of concrete specimens under cyclic loading, as discussed later.

Crack-Closing Model

A number of researchers studied the behavior of concrete during tension-compression transitions. Ramtani et al. (1992), for example, observed that the tensile cracks did not completely close as the concrete unloaded from tension toward compression. This behavior was attributed to shear slippage across the cracked surfaces and led to the presence of residual tensile deformations. Ramtani et al. (1992) also observed that crack closure may occur at a certain level of compressive stress and that the stiffness of concrete in compression was fully recovered at that level and not affected by the damage incurred in the previous tension cycle. Palermo and Vecchio (2003), Légeron et al. (2005), and Sima et al. (2008) attempted to incorporate the crack-closing behavior in uniaxial rule-based concrete models, among others. However, the crack-closing behavior in uniaxial concrete models is not well-characterized due to the lack of experimental observations. This deficiency may be attributed to the difficulty of conducting experimental tests with tension-compression transitions. As a result, the available uniaxial models that incorporate the crack-closing behavior remain difficult to calibrate.

The following model is proposed to characterize the crack-closing response as the material stress state transitions from tension to compression. This model is only activated after the material has experienced plastic tensile strain, representing the presence of tensile cracks. Crack closure is accommodated by introducing additional compressive plastic strains during the tension-compression transition. These plastic strains continue to evolve only as long

as the cracks are open (i.e., as long as the tensile plastic strain is larger than zero). The model resembles an additional plasticity model that is nested into the main plasticity framework and is only valid under the following conditions:

- The material has experienced tensile plastic deformations at some point during the load history, and these deformations remain larger than zero, meaning that tensile cracks are not fully closed yet.
- The material is experiencing compressive stress (i.e., crack-closing is occurring at the current material state).

The additional plastic strains experienced by the material ε_k^p are called crack-closing strains, and the crack-closing model is distinguished from the main plasticity model by the subscript k. An internal variable is postulated for the crack-closing evolution. This variable is assumed to evolve according to the following expression:

$$\dot{k}_k = |\dot{\varepsilon}_k^p| \tag{27}$$

and the following stress-strain law (in rate form), flow rule, yield function, and consistency conditions hold, respectively:

$$\dot{\bar{\sigma}} = E(\dot{\varepsilon} - \dot{\varepsilon}_k^p) \tag{28}$$

$$\dot{\varepsilon}_k^p = \dot{\lambda} \tag{29}$$

$$f_k = |\bar{\sigma}| - \sigma_k(k_k) \tag{30}$$

$$f_k \le 0,\ \dot{\lambda} \ge 0,\ \dot{\lambda} f_k = 0 \tag{31}$$

such that the evolution of the crack-closing stress σ_k (which is analogous to the yield stress) is described by

$$\sigma_k(k_k) = H_k k_k \tag{32}$$

Note that Eq. (28) implicitly assumes that the evolution of crack-closing plastic strains may not occur simultaneously with the plasticity evolution in the main model. This restriction means that the tensile cracks are assumed to fully close during the elastic reloading phase in compression.

Eq. (32) illustrates that the rate at which crack closure takes place is controlled by the modulus H_k. In particular, H_k controls the decomposition of the compressive strain increment into an elastic strain increment and a plastic strain increment that contributes to the closing of the tensile cracks. For example, a value of $H_k = 0.0$ means that the behavior is perfectly plastic, i.e., all of the compressive strain experienced by the material is plastic crack-closing strain (until the cracks are fully closed). The adopted crack-closing mechanism is shown in the full compression-tension cycles depicted in Fig. 2 for two different values of H_k (the tensile capacity of concrete is not to scale).

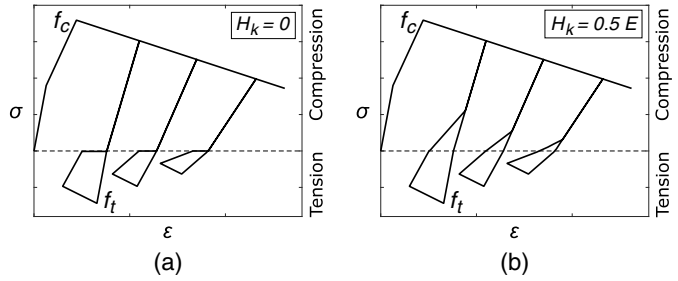

Fig. 2. Effect of the modulus H_k on the crack-closing rate: (a) $H_k = 0$; and (b) $H_d = 0.5E$.

Nonlocal Damage Model

Nonlocal Averaging Concept

In the integral nonlocal approach, a local field variable $f(x)$ at a location x is replaced by its nonlocal counterpart $\widetilde{f(x)}$, which is evaluated as a weighted average of the local variable over a spatial neighborhood of that location. In the one-dimensional context, this averaging procedure may be expressed as

$$\widetilde{f(x)} = \int_L \bar{w}(x, r) f(r) dr \tag{33}$$

where L = length of the spatial averaging domain; $\bar{w}(x, r)$ = weighting function that satisfies the normalizing condition, such that the nonlocal averaging operator does not alter a uniform field. This normalization may be expressed as

$$\bar{w}(x, r) = \frac{w(x, r)}{\int_L w(x, r) dr} \tag{34}$$

The value of the weight function $w(x, r)$ depends solely on the distance between the two spatial locations, which is represented by the local coordinate of a neighboring point r. The choice of the weight function controls the size of the localization zone and the strain distribution within the zone. A bell-shaped function is conventionally used as the weight function, for example

$$w(r) = \left\langle 1 - \frac{r^2}{R^2} \right\rangle^2 \tag{35}$$

where R = interaction radius that is related or equivalent to the characteristic length of the nonlocal model; and the Macaulay brackets $\langle \ldots \rangle$ indicate only the positive part of the argument.

Nonlocal Compression Damage

In the nonlocal version of the model, the material damage state at a Gauss point is assumed to depend on the material state in the neighboring Gauss points within multiple elements, whereas the plasticity state remains local. This approach results in a more computationally efficient formulation (compared to nonlocal plasticity) since the plasticity part, which is generally implicit and may require iteration, is local, and the nonlocality in enforced in the explicit damage part. The selected state variable for nonlocal averaging is the compression damage history variable k_{dc}. Therefore, the rate of the nonlocal variable $\widetilde{k_{dc}}$ may be expressed as

$$\dot{\widetilde{k_{dc}}}(x) = \int_L \bar{w}(x, r) \dot{k}_{dc}(r) dr \tag{36}$$

where $k_{dc}(r)$ = compression damage variable at a Gauss point that is a distance r away from point x. Accordingly, the damage parameter D_c may be evaluated as follows:

$$D_c(\widetilde{k_{dc}}) = \frac{E\widetilde{k_{dc}}(H_d(\varepsilon_f - k_0) + f_c)}{(f_c + H_d\widetilde{k_{dc}})(E(\varepsilon_f - k_0) - f_c)} \tag{37}$$

Eqs. (36) and (37) indicate that evaluating the damage parameter requires knowledge of the increments of the damage variable k_{dc} in multiple Gauss points surrounding the current point. This issue is discussed further within the numerical implementation procedure.

Nonlocal Tension Damage

A similar nonlocal approach is followed for the tension damage evolution, leading to the following expression for the rate of the nonlocal tension damage history variable:

$$\dot{\widetilde{k_{dt}}}(x) = \int_L \bar{w}(x,r)\dot{k}_{dt}(r)dr \tag{38}$$

and the tensile damage parameter is evaluated using $\widetilde{k_{dt}}$

$$D(\widetilde{k_{dt}}) = \frac{E\widetilde{k_{dt}}(H_d\varepsilon_{ft} + f_t)}{(f_t + H_d\widetilde{k_{dt}})(E\varepsilon_{ft} - f_t)} \tag{39}$$

Model Parameters and Numerical Implementation

Description of the Model Parameters

The model response under compressive stress is controlled by six parameters: elastic modulus E, peak compressive stress f_c, strain at the peak compressive stress ε_{co}, initial yield stress f_y, softening slope (slope of the descending branch) E_d, and secondary plastic modulus H_d. Under tensile stress, the model is controlled by the tensile strength f_t, strain at zero stress ε_{ft}, and plastic modulus H_t. Finally, the crack-closing behavior of the model is controlled by the modulus H_k. The parameters E, f_c, ε_{co}, f_y, E_d, f_t, and ε_{ft} may be directly obtained from the monotonic uniaxial stress-strain response of concrete. The moduli H_d, H_t, and H_k are specific to the proposed damage and crack-closing frameworks and are studied more thoroughly. The following recommendations are made for obtaining the necessary model parameters:

- The elastic modulus, peak compressive stress, and strain at the peak compressive stress are assumed to be known values for plain (unconfined) concrete. Based on experimental evidence, the compressive stress in plain concrete typically vanishes at a strain value ε_f between 0.005 and 0.01 from which the descending slope E_d can be calculated.
- The proposed model is intended for use in FD frame models for the analysis of RC beam-columns. Therefore, the confining effect of the transverse steel reinforcement in the column on the properties of the concrete must be considered. In fiber-based simulations, this confining effect is typically taken into account by enhancing the properties of the underlying concrete material model, namely, the peak compressive stress, strain at the peak compressive stress, and softening slope. Estimates of the enhanced properties of the confined concrete are provided by several models in the literature that vary in simplicity, range of applicability, and accuracy (e.g., Scott et al. 1982; Mander et al. 1988; Sheikh and Uzumeri 1982; Razvi and Saatcioglu 1999). The authors studied the predictions of a number of these models in earlier work (Kenawy et al. 2018) and concluded that it was difficult to find a model that consistently produced accurate predictions across different specimens. In this study, the modified Kent–Park model (Scott et al. 1982) is used to estimate the properties of confined concrete. While determining these properties is outside the scope this work, the softening slope of the confined concrete is one of the main parameters controlling the strength degradation of RC beam-columns. Consequently, inaccurate estimation of this slope may significantly affect the predictions of the proposed model. This issue will be further discussed in reference to the results of this study.
- The initial yield stress f_y determines the limit of the elastic response of the concrete under compression and is typically observed during uniaxial compression tests to be in the range of 30%–60% of the peak compressive stress. In the current study, f_y is assumed to be 50% of the peak compressive stress f_c.
- The secondary plastic modulus H_d, which was discussed in the preceding section, represents an indirect measure of the stiffness degradation of the material under compressive stress. The parameter H_d is difficult to calibrate precisely because the unloading/reloading stiffness within each loading cycle is assumed to be constant in the model; i.e., the observed variation in stiffness within a single cycle during experimental tests is ignored. This variation, however, has only a modest effect on the overall response of RC beam-columns, as discussed in the results section. A general value for the plastic modulus H_d of 15% of the elastic modulus E is recommended and used in the current study for all simulations. This value was obtained by comparing the cyclic stress-strain response predicted by the proposed model with that of plain concrete specimens tested by Sinha et al. (1964), Karsan and Jirsa (1969) and Okamoto et al. (1976). Fig. 3 shows the predicted unloading/reloading by the model using the recommended value of H_d on top of the corresponding experimental observations.
- Other parameters that control the monotonic compressive response may be derived from the preceding parameters. The value of the plastic strain at the peak stress k_0, the plastic modulus H, and the magnitude of the final total strain ε_f (strain at zero stress) are calculated as follows:

$$k_0 = \varepsilon_{co} - \frac{f_c}{E} \tag{40}$$

$$H = \frac{f_c - f_y}{k_0} \tag{41}$$

$$\varepsilon_f = \varepsilon_{co} - \frac{f_c}{E_d} \tag{42}$$

  where ε_{co}, f_y, and f_c are all positive values.
- The tensile strength f_t is assumed to be equal to 10% of the peak compressive stress, and ε_{ft} is assumed to be in the range 0.003–0.005. The plastic modulus H_t is analogous to the modulus H_d in compression. Therefore, it requires calibration based on the stiffness degradation observed during strain reversal under tensile stress. However, such calibrations were not performed in the current study, and the value of H_t is assumed to be identical to the value of H_d: $0.15E$. Similarly, the plastic modulus for crack closure H_k requires calibration based on experimental observations of the crack-closing behavior under uniaxial mixed compression-tension cycles. However, such measurements are scarce in the literature. A value for H_k equal to $0.05E$ was seen to achieve a reasonable agreement with the overall hysteretic response of the RC columns studied herein.

Nonlocal Length Scale

In a nonlocal continuum, a finite strain localization zone is enforced by considering interactions between neighboring material points within a prescribed length scale. Theoretically, this scale may represent a characteristic length of the material, which may be informed by the heterogeneity of the microstructure, e.g., the maximum aggregate size in concrete (Bažant 1976; Bažant and Pijaudier-Cabot 1989). At the scale of structural members, the length scale of a nonlocal model has conventionally been considered to be the same as the localization length or the length over which the member inelastic deformations localize. This interpretation is convenient because it allows the nonlocal local length scale

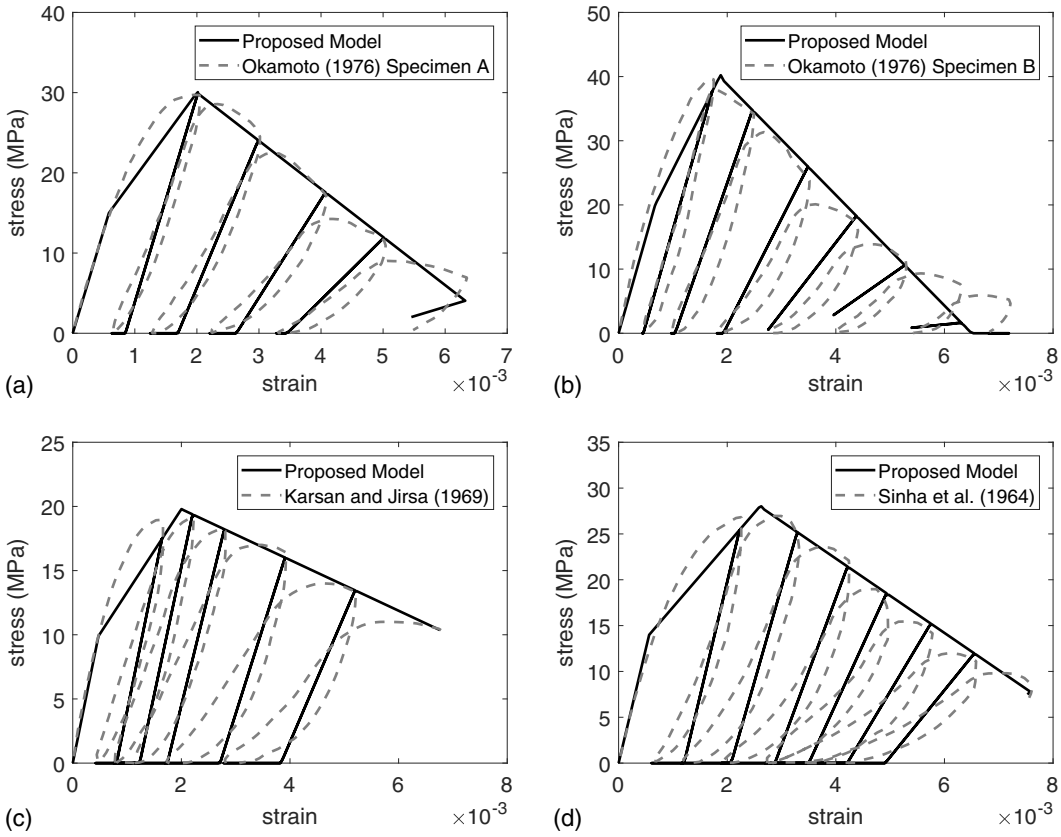

Fig. 3. Predicted and observed cyclic stress-strain response for the following plain concrete specimens tested: (a) Okamoto et al. (1976), Specimen A; (b) Okamoto et al. (1976), Specimen B; (c) Karsan and Jirsa (1969); and (d) Sinha et al. (1964).

to be approximated as a fraction of the beam length or as the cross sectional dimension, in an equivalent sense to the plastic hinge length that has been adopted for decades (Paulay and Priestley 1992). Such an approach has been used in the studies by Salehi and Sideris (2017) and Valipour and Foster (2009). In this study, however, we do not directly regularize the sectional deformations of the beam element. Consequently, we do not enforce a plastic-hinge length on the structural member, as was done previously. Instead, we indirectly regularize the beam sectional deformations by enforcing nonlocal interaction in the uniaxial constitutive response of individual cross sectional fibers. Therefore, we deemed it both appropriate and convenient to select a nonlocal length scale that is associated with the constitutive model, rather than the cross sectional dimensions.

From the perspective of uniaxial constitutive models, it is well known that the measured slope of the softening regime of the stress-strain response of the material is dependent on the size of the underlying test specimen (e.g., Markeset and Hillerborg 1995). This implies that at the scale of a structural member, where the inelastic deformations clearly localize in a region of a certain size (i.e., during softening), the measured strains depend on the size of the region over which the measurements are performed (often referred to as the gauge length). In this sense, the slope of the softening curve of concrete (at a structural member scale) may be regarded as a function of the measuring gauge length. In light of this interpretation and the nature of the proposed nonlocal approach, we proposed the use of the measuring gauge length in an experiment as the length scale of the nonlocal interaction in the model (Kenawy et al. 2018). This proposal was intended to account for the influence of the microstructure in an approximate, averaged-out sense. For example, if a plain concrete member is subjected to pure compressive loading, and the stress-strain curve is determined by measuring axial deformation over a length R of the member, then it is possible to reproduce the same stress-strain response in a numerical analysis using the proposed nonlocal model with a nonlocal length scale of R. In other words, the proposed nonlocal approach may be visualized to diffuse or distribute the damage over this gauge length to achieve consistency with experimental measurements.

The preceding interpretation implies that, at least theoretically, the length scale of the proposed nonlocal approach may be obtained directly from uniaxial experimental tests. The difficulty with this approach, however, is that the tests would need to be conducted on components with similar sizes to the structural members of interest to the analysis, which is impractical in most cases. This difficulty is overcome by recognizing that the softening slope of the core concrete fibers in structural analysis of RC members is typically determined using certain confinement models [such as Scott et al. (1982), Mander et al. (1988), and Sheikh and Uzumeri (1982)]. Such confinement models consist of equations that follow from statistical regression over a large suite of uniaxial compression tests on RC column specimens. Therefore, the experimental tests behind a certain confinement model provide the appropriate length scale associated with the predicted stress-strain relationship by the model (specifically, the predicted softening slope). With this understanding, the modified Kent–Park confinement model (Scott et al. 1982) was used in this study, and the gauge length in the Kent–Park test specimens was used as the nonlocal length scale. This selection is somewhat arbitrary, as several confinement models provide reasonable predictions [although no single model performs consistently well across specimens from different studies,

as demonstrated in Kenawy et al. (2018)]. Therefore, other confinement models can be used to estimate the softening slope of the confined concrete (as an input to the material model), with their associated gauge length to act as the nonlocal scale. It is important to note that the inherent size effects associated with the selected confinement model (because of the size of the specimens used in deriving the model) may still be present. However, this issue is an artifact of the underlying models and is outside the scope of this study. The proposed interpretation of the macroscopic length scale is seen to reproduce, with good accuracy, the observed behavior of all the specimens investigated in this study.

It is emphasized that the proposed approach does not directly enforce a plastic hinge length onto the model; i.e., the length over which the section curvatures would localize is not determined a priori. This feature is a byproduct of imposing the nonlocality on the constitutive relationships of individual fibers, rather than the section deformations. While this approach may be regarded as an approximate representation of the localization in structural members, it was shown in Kenawy et al. (2018) to agree reasonably well with available experimental data of member curvature distributions. More test data is needed, however, to verify the validity of this approach for a wider range of member sizes and cross sectional dimensions. It is also recognized that the shear span-depth ratio of the structural member (the ratio of the effective length L to the cross section depth d) may play a role in determining the appropriate nonlocal length scale, which was not detected in the specimens analyzed in this study (which have cross sectional dimensions between 250 and 550 mm, and L/d ratios between 2.6 and 5.5). Further studies on larger columns with different L/d ratios are necessary to properly quantify that effect. As an alternative proposal, and based solely on the specimens studied herein, reasonable agreement with experimental observations would also be obtained if the nonlocal length scale is expressed as

$$R = 100\frac{L}{d}\ (\text{mm}) \tag{43}$$

Algorithmic Implementation

The proposed nonlocal model for concrete is implemented in the structural analysis platform OpenSees (McKenna et al. 2000). The model is combined with the nonlocal displacement-based element formulation previously developed by the authors. Fig. 4 provides a schematic representation of the nonlocal analysis methodology, incorporating the nonlocal displacement-based element, which is described in detail in Kenawy et al. (2018). The algorithmic implementation of the constitutive model has the following three major components:

1. The plasticity part, which is typically treated in an incremental form. A numerical scheme (e.g., return mapping algorithm) and an iterative procedure are generally required to solve the plasticity equations for the effective stress increment $\Delta\bar{\sigma}$, the increment of the plastic multiplier $\Delta\lambda$, and the internal variables k_c and k_t. In the current one-dimensional form of the model, the solution to the plasticity problem follows the standard operator splitting into two steps: elastic step (predictor) and plastic step (corrector). Because of the linearity of the hardening law in Eqs. (10) and (11), the incremental plasticity equations can be solved analytically. For a more sophisticated evolution of hardening [for example, using the third-order polynomial in Grassl and Jirásek (2006)], solving the plasticity problem requires an iterative scheme; the details of which are available elsewhere (e.g., Saritas and Filippou 2009). The plasticity part is assumed to be local in the current model; i.e., the solution at a material point depends only on the state at that point, and no interaction between neighboring points is considered.
2. The damage part in which the evolution of the damage variables is linked to the evolution of the plastic strain, and these variables can be updated after solving the plasticity problem. In the nonlocal form of the damage model, the damage parameters D_c and D_t are evaluated based on the nonlocal damage variables (in compression or tension) using Eqs. (37) and (39). As expressed in Eqs. (36) and (38), this operation requires knowledge of the damage variable increments in the neighboring material points. From the implementation point of view, transferring this data between different material points increases the computational effort significantly and is inconvenient from the perspective of modern object-oriented FE codes. The computational effort can be largely reduced by making a suitable approximation of the nonlocal damage variables $\widetilde{k_{dc}}$ and $\widetilde{k_{dt}}$. To arrive at this approximation for compressive damage, Eqs. (12) and (19) are substituted into Eq. (36), and the plastic strain increment is replaced by the difference between the total and elastic strain increments, leading to the following expression:

$$\dot{\widetilde{k_{dc}}}(x) = (1-\alpha)\int_L \bar{w}(x,r)|\dot{\varepsilon}(r) - \dot{\varepsilon}^e(r)|dr \quad \text{if } k_c > k_0 \tag{44}$$

Because no softening is allowed in the plasticity model, the total and elastic strain increments have the same sign during plastic loading. Therefore, Eq. (44) may be rewritten as

$$\begin{aligned}\dot{\widetilde{k_{dc}}}(x) &= (1-\alpha)\left(\int_L \bar{w}(x,r)|\dot{\varepsilon}(r)|dr - \int_L \bar{w}(x,r)|\dot{\varepsilon}^e(r)|dr\right)\\ &= (1-\alpha)(|\dot{\bar{\varepsilon}}(x)| - |\dot{\bar{\varepsilon}}^e(x)|)\end{aligned} \tag{45}$$

Note that the preceding equation implicitly assumes that the strains at the material points within the nonlocal averaging

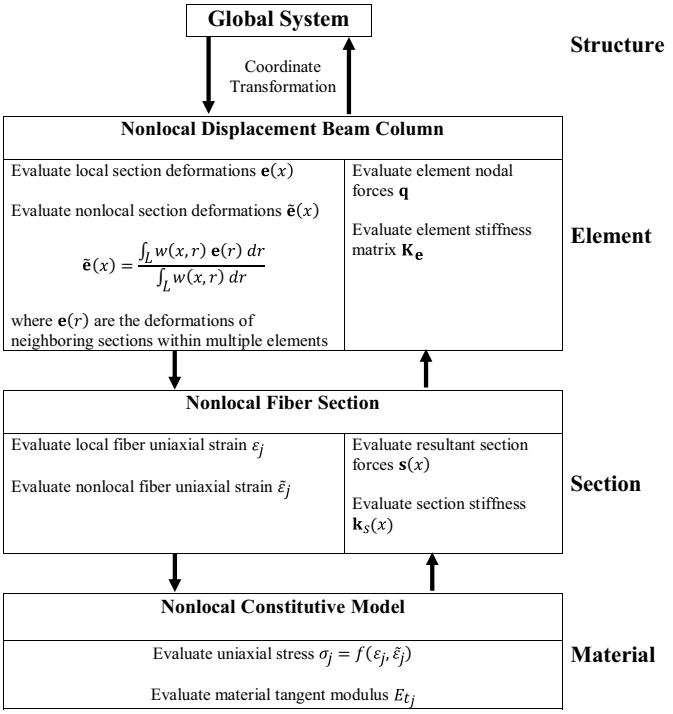

Fig. 4. Schematic implementation of the nonlocal fiber-based framework.

domain have the same sign. At this point, the magnitude of the nonlocal elastic strain increment in Eq. (45) is approximated by the local elastic strain increment, i.e.

$$|\dot{\varepsilon}^e(x)| \approx |\dot{\bar{\varepsilon}}^e(x)| = \int_L \bar{w}(x,r)|\dot{\varepsilon}^e(r)|dr \tag{46}$$

allowing for the equation to be rewritten as

$$\dot{\tilde{k}}_{dc}(x) = (1-\alpha)(|\dot{\bar{\varepsilon}}(x)| - |\dot{\varepsilon}^e(x)|) \tag{47}$$

In a similar fashion, the following approximate expression for the rate of the nonlocal tension damage variable can be obtained:

$$\dot{\tilde{k}}_{dt}(x) = \alpha(|\dot{\bar{\varepsilon}}(x)| - |\dot{\varepsilon}^e(x)|) \tag{48}$$

and the following observations can be made:

- Eqs. (47) and (48) utilize the nonlocal total strain increment at the material point (in lieu of the nonlocal plastic strain increment) to compute the nonlocal damage variable. This replacement greatly reduces the required computational effort because the total strain increment depends only on the applied nodal displacements and is evaluated at the level of the element cross-sections (as described in Fig. 4).
- Eqs. (47) and (48) are only exact if the elastic strain increment is uniform within the nonlocal averaging region. However, due to the fact that the plastic strain is much larger than the elastic strain during the softening phase, this approximation has a negligible effect on the computed value of the nonlocal damage variables. An equivalent approach was proposed in the nonlocal formulation of Brinkgreve (1994) for geomaterials.
- The approximations in Eqs. (46)–(48) are only used for computing an approximate value of the nonlocal damage variables for the purpose of evaluating the damage parameter and are not used to replace the current elastic strain increment at the material point. Similarly, these equations clarify that the nonlocal strain evaluated at the cross section level in Fig. 4 is only used to control the evolution of damage and does not replace the current value of the local total strain.
- Eqs. (47) and (48) may only be applied during plastic loading (i.e., when the increments of the total, plastic, and elastic strains have the same sign) and cannot be applied during unloading.

Following the application of Eqs. (47) and (48), the damage parameter can be evaluated using Eqs. (37), (39), and (14), and the nominal stress can be evaluated using Eq. (2).

3. The crack-closing part is only activated in the analysis if the material is loading under compressive stress, and has accumulated tensile plastic strains at some point during the loading history. The crack-closing part is, in concept, a hardening plasticity model during which additional compressive plastic strains are accumulated until the existing tensile plastic strains are diminished. The crack-closing evolution is assumed to be linear in the present model; therefore, the equations of this additional plasticity model can be conveniently solved analytically.

The algorithmic implementation of the constitutive model is presented in Fig. 5. The equations in the figure represent a typical analysis step at time $n+1$ where the constitutive quantities are known at time n. In addition, the value of the strain is known at time $n+1$ and is used to recover the nominal stress σ_{n+1}. It is noted that the plasticity equations [the incremental versions of Eqs. (1), (4), (5), (12), and (13)] are solved analytically in Step 4, in which the effective plastic modulus is the following:

$$H_{eff} = (1-\alpha)^2 H_c + \alpha^2 H_t \tag{49}$$

where H_c = plasticity modulus under compressive stress, which depends on whether the material is in the hardening or softening phase

$$H_c = \begin{cases} H & \text{if } k_c \le k_0 \\ H_d & \text{if } k_c > k_0 \end{cases} \tag{50}$$

and H_t = plasticity modulus defined earlier for the tensile response.

Performance of the Proposed Constitutive Model

Several numerical studies were conducted to examine the ability of the proposed model to simulate the post-peak response of cantilever RC beam-columns subjected to a combination of constant axial and cyclic lateral loads at the free end, as shown in Fig. 6(a). First, the mesh convergence of the nonlocal model was studied in a pushover analysis context. Then, the predicted cyclic RC column response by the nonlocal model was compared against (1) the predicted response by the local model, and (2) the observed column response during experimental tests. It is noted that the same nonlocal displacement-based element formulation is used in combination with both the local and nonlocal versions of the material model. However, the nonlocality in the model is only activated when the nonlocal section deformations computed at the element level are used by the nonlocal material model to determine the damage variable. In other words, no nonlocal regularization is enforced in the model if the material model uses a local measure of the damage variable. Table 1 presents a database of 24 RC columns from 10 different experimental studies, which were used as benchmark data for validating the performance of the nonlocal model. The load-displacement response of each specimen was obtained from the PEER column database (Berry et al. 2004). All specimens were subjected to constant axial load and quasi-static lateral displacement cycles and were reported to fail in flexure. The specimens span a practical range of interest for shear span-depth ratios (the cantilever length L divided by the section depth d), axial load ratios (denoting the ratio of the axial load applied to the column P to its nominal axial capacity $f_c A_g$), and transverse steel reinforcement ratios ρ_t. Each specimen was simulated by three numerical models that were created using OpenSees. The first simulation model was created using the proposed constitutive framework combined with the nonlocal frame element (Kenawy et al. 2018); this model is henceforth referred to as the nonlocal DPTC model. To isolate the effects of the tensile behavior properties and proposed crack-closing mechanism, the second simulation model (referred to as the nonlocal DPC model) was created also using the proposed nonlocal approach, but with suppressed tensile capacity (f_t is assumed to be zero), and a zero crack-closing modulus; i.e., this simulation model represents the compressive behavior of the material only. The third model (referred to as the local model) was created using a local version of the proposed damage-plasticity formulation [i.e., the damage evolution is controlled by the local damage parameters evaluated using Eqs. (24) and (26)], combined with the same element formulation.

Each structural member was modeled as a series of frame elements with the Gauss Legendre integration rule and two integration points per element. A fiber cross-section was defined at each integration point and consisted of three distinct materials: unconfined (plain) concrete for the cover, confined concrete (with enhanced strength and strength degradation properties) for the core, and

Step 1. Elastic predictor

plastic strain $\varepsilon^{p}_{n+1} = \varepsilon^{p}_{n}$
trial stress $\overline{\sigma}^{tr}_{n+1} = E\left(\varepsilon_{n+1} - \varepsilon^{p}_{n+1}\right)$
if $\overline{\sigma}^{tr}_{n+1} > 0.0$
  $\alpha = 1.0$
  else
  $\alpha = 0.0$

Step 2. Crack-closing plasticity

if $\overline{\sigma}^{tr}_{n+1} < 0.0$ and $\Delta\varepsilon_{n+1} < 0.0$ and $k_{tn} + k_{kn} > 0.0$
  activate crack-closing plasticity:
  crack-closing plastic strain increment $\Delta\varepsilon^{p}_{kn+1} = \frac{E}{E+H_k}\Delta\varepsilon_{n+1}$
  plastic strain $\varepsilon^{p}_{n+1} \leftarrow \varepsilon^{p}_{n+1} + \Delta\varepsilon^{p}_{kn+1}$
  crack-closing history variable $k_{kn+1} = k_{kn} + \Delta\varepsilon^{p}_{kn+1}$
  trial stress $\overline{\sigma}^{tr}_{n+1} \leftarrow \overline{\sigma}^{tr}_{n+1} - E\Delta\varepsilon^{p}_{kn+1}$

Step 3. Evaluate the yield function

$f = \left|\overline{\sigma}^{tr}_{n+1}\right| - \sigma_{yc}\left(k_{cn}\right) + \alpha\left(\sigma_{yc}\left(k_{cn}\right) - \sigma_{yt}\left(k_{tn}\right)\right)$
if $f < 0.0$
  effective stress $\overline{\sigma}_{n+1} = \overline{\sigma}^{tr}_{n+1}$
  compression damage parameter $D_{cn+1} = D_{cn}$
  tension damage parameter $D_{tn+1} = D_{tn}$
  move to step 6
else
  continue to step 4

Step 4. Plastic corrector

increment of plastic multiplier $\Delta\lambda = \frac{f}{E+H_{eff}}$
plastic strain $\varepsilon^{p}_{n+1} \leftarrow \varepsilon^{p}_{n+1} + \Delta\lambda\ sign\left(\overline{\sigma}^{tr}_{n+1}\right)$
compression history variable $k_{cn+1} = k_{cn} + (1-\alpha)\Delta\lambda$
tension history variable $k_{tn+1} = k_{tn} + \alpha\Delta\lambda$
effective stress $\overline{\sigma}_{n+1} = \overline{\sigma}^{tr}_{n+1} - E\Delta\lambda\ sign\left(\overline{\sigma}^{tr}_{n+1}\right)$

Step 5. Evaluate nonlocal damage

nonlocal compression damage history variable $\widetilde{k_{dcn+1}} = \widetilde{k_{dcn}} + (1-\alpha)\left(\left|\Delta\widetilde{\varepsilon}_{n+1}\right| - \left|\Delta\varepsilon^{e}_{n+1}\right|\right)$
compression damage parameter $D_{cn+1} = \frac{E\,\widetilde{k_{dcn+1}}\left(H_d\left(\varepsilon_f - k_0\right) + f_c\right)}{\left(f_c + H_d\widetilde{k_{dcn+1}}\right)\left(E\left(\varepsilon_f - k_0\right) - f_c\right)}$
nonlocal tension damage history variable $\widetilde{k_{dtn+1}} = \widetilde{k_{dtn}} + \alpha\left(\left|\Delta\widetilde{\varepsilon}_{n+1}\right| - \left|\Delta\varepsilon^{e}_{n+1}\right|\right)$
tension damage parameter $D_{tn+1} = \frac{E\,\widetilde{k_{dtn+1}}\left(H_d\varepsilon_{ft} + f_t\right)}{\left(f_t + H_d\widetilde{k_{dtn+1}}\right)\left(E\varepsilon_{ft} - f_t\right)}$

Step 6. Damage corrector

damage parameter $D_{n+1} = (1-\alpha)\,D_{cn+1} + \alpha D_{tn+1}$
nominal stress $\sigma_{n+1} = (1 - D_{n+1})\,\overline{\sigma}_{n+1}$

Fig. 5. Algorithmic implementation of the nonlocal constitutive model.

reinforcing steel. The model parameters for the unconfined and confined concrete were obtained, as discussed in the preceding section. The modified Kent–Park confinement model (Scott et al. 1982) was used to estimate the peak compressive stress and softening slope of the confined concrete. The gauge length associated with the confinement model was used as the length scale of the nonlocal model for all specimens. For the Kent–Park model, this gauge length was reported as 400 mm. The properties of the longitudinal steel reinforcement (the elastic modulus E_s, the yield stress f_y, the hardening ratio b or ratio between the elastic modulus and post-yield modulus) were typically provided for each specimen. Steel02 model in OpenSees (Menegotto and Pinto 1973) was used for simulating the behavior of the steel rebar and is shown in Fig. 6(b). It is noted that three-dimensional failure mechanisms associated with the steel rebar (buckling or fracture) are not considered in these models. A discussion of the effect of these failure modes on the post-peak response of RC columns is presented later. Representative results of the numerical studies are presented in the following subsections.

Mesh Sensitivity of the Local and Nonlocal Models under Monotonic Displacements

The sensitivity of both the local and nonlocal model predictions to the FE mesh size is studied in a pushover simulation of specimen #17. The number of elements along the member was varied parametrically between 4 and 18 elements, and several response quantities were recorded to monitor the global and local member response. The global response is represented by the lateral load versus lateral displacement at the free end, whereas the local response

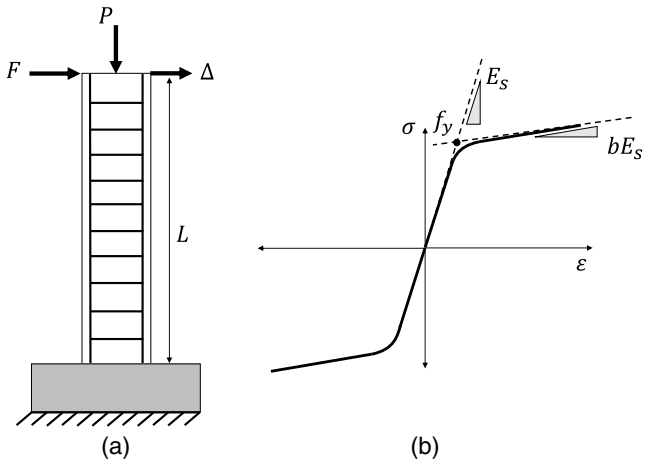

Fig. 6. Properties of the simulation models: (a) geometric configuration and loading of the test problem; and (b) behavior of the reinforcing steel.

is represented by the curvature at each cross section (or Gauss point) along the member.

Figs. 7(a and b) display the predicted load versus drift ratio (lateral displacement normalized by the cantilever length) for specimen #17 predicted by a local and a nonlocal version of the DPTC model, respectively, using the different mesh refinements, whereas Figs. 7(c and d) display the curvature profile along the member for both models. The local and nonlocal model results are plotted for the same mesh sizes. The local model simulations are identified by the number of FEs along the member, and the nonlocal model simulations are identified by the ratio of the element size to the nonlocal length scale (which is constant for all simulations). Fig. 7(b) shows that the global response predictions of the nonlocal model rapidly converge as the mesh is refined such that the load-displacement response predicted using a mesh size of 8 elements is identical to the predictions of the 18-element mesh, whereas the predicted post-peak response by the local model pathologically depends on the mesh size. The same conclusion is affirmed by comparing subplots c and d featuring the curvature distribution predicted by both models. Importantly, Fig. 7(d) shows that capturing the nonlinear distribution of the curvature along the member requires a relatively fine mesh, particularly near the critical section at the base of the member, which is a standard requirement for displacement-based frame elements. In all nonlocal simulations, however, the pathological mesh sensitivity is eliminated, and the nonlocal averaging operation is effective even when the element size is equal to the nonlocal length scale. These results suggest that the proposed nonlocal approach and associated interpretation of the length scale do not impose stringent restrictions on the FE mesh size. In fact, the mesh refinement requirements imposed by the need to accurately capture the nonlinear deformation field are expected to govern for the scale of the structural members considered in this study.

Another important point of comparison between the local and nonlocal models is the moment-curvature response at the cross section level. Fig. 8 displays the moment-curvature response, corresponding to the results shown in Fig. 7, at the column base (first integration point) for mesh sizes of 6, 10, and 16 elements. Figs. 8(a and b) show the predictions of the local and nonlocal models, respectively, whereas Fig. 8(c) overlays the predictions of the 16-element mesh using both the local and nonlocal models. The results in Fig. 8 suggest the following:

- As the mesh size is refined, the maximum curvature at the column base predicted by the local model is generally expected to be much higher than that predicted by the nonlocal model. This result is due to the localization of the inelastic curvature at the

Table 1. Properties of the benchmark column specimens

Specimen number	Reference	Length, L (mm)	Section depth, d (mm)	Axial load ratio, $\eta = \frac{P}{f_c A_g}$	Unconfined concrete strength, f_c (MPa)	Transverse reinf. ratio, ρ_t	Longitudinal reinf. ratio, ρ_l
1	Ang et al. (1981), No. 3	1,600	400	0.38	23.6	0.028	0.015
2	Ang et al. (1981), No. 4	1,600	400	0.21	25.0	0.022	0.015
3	Atalay and Penzien (1975), No. 11	1,676	305	0.28	31.0	0.015	0.016
4	Atalay and Penzien (1975), No. 10	1,676	305	0.27	32.4	0.009	0.016
5	Atalay and Penzien (1975), No. 6S1	1,676	305	0.18	31.8	0.009	0.016
6	Gill et al. (1979), No. 1	1,200	550	0.26	23.1	0.015	0.018
7	Gill et al. (1979), No. 3	1,200	550	0.42	21.4	0.018	0.018
8	Kanda et al. (1988), 85STC-1	750	250	0.11	27.9	0.011	0.016
9	Kono and Watanabe (2000), D1N60	625	242	0.66	37.6	0.015	0.024
10	Kono and Watanabe (2000), D1N30	625	242	0.33	37.6	0.015	0.024
11	Saatcioglu and Grira (1999), BG-1	1,645	350	0.43	34.0	0.010	0.020
12	Saatcioglu and Grira (1999), BG-2	1,645	350	0.43	34.0	0.020	0.020
13	Saatcioglu and Grira (1999), BG-3	1,645	350	0.20	34.0	0.020	0.020
14	Saatcioglu and Grira (1999), BG-4	1,645	350	0.46	34.0	0.013	0.029
15	Saatcioglu and Grira (1999), BG-8	1,645	350	0.23	34.0	0.013	0.029
16	Soesianawati et al. (1986), No. 1	1,600	400	0.10	46.5	0.009	0.015
17	Soesianawati et al. (1986), No. 2	1,600	400	0.30	44.0	0.012	0.015
18	Soesianawati et al. (1986), No. 3	1,600	400	0.30	44.0	0.008	0.015
19	Soesianawati et al. (1986), No. 4	1,600	400	0.30	40.0	0.006	0.015
20	Tanaka and Park (1990), No. 1	1,600	400	0.20	25.6	0.026	0.016
21	Tanaka and Park (1990), No. 7	1,650	550	0.30	32.1	0.021	0.013
22	Watson and Park (1989), No. 5	1,600	400	0.50	41.0	0.014	0.015
23	Watson and Park (1989), No. 9	1,600	400	0.70	40.0	0.048	0.015
24	Zahn et al. (1985), No. 7	1,600	400	0.22	28.3	0.016	0.015

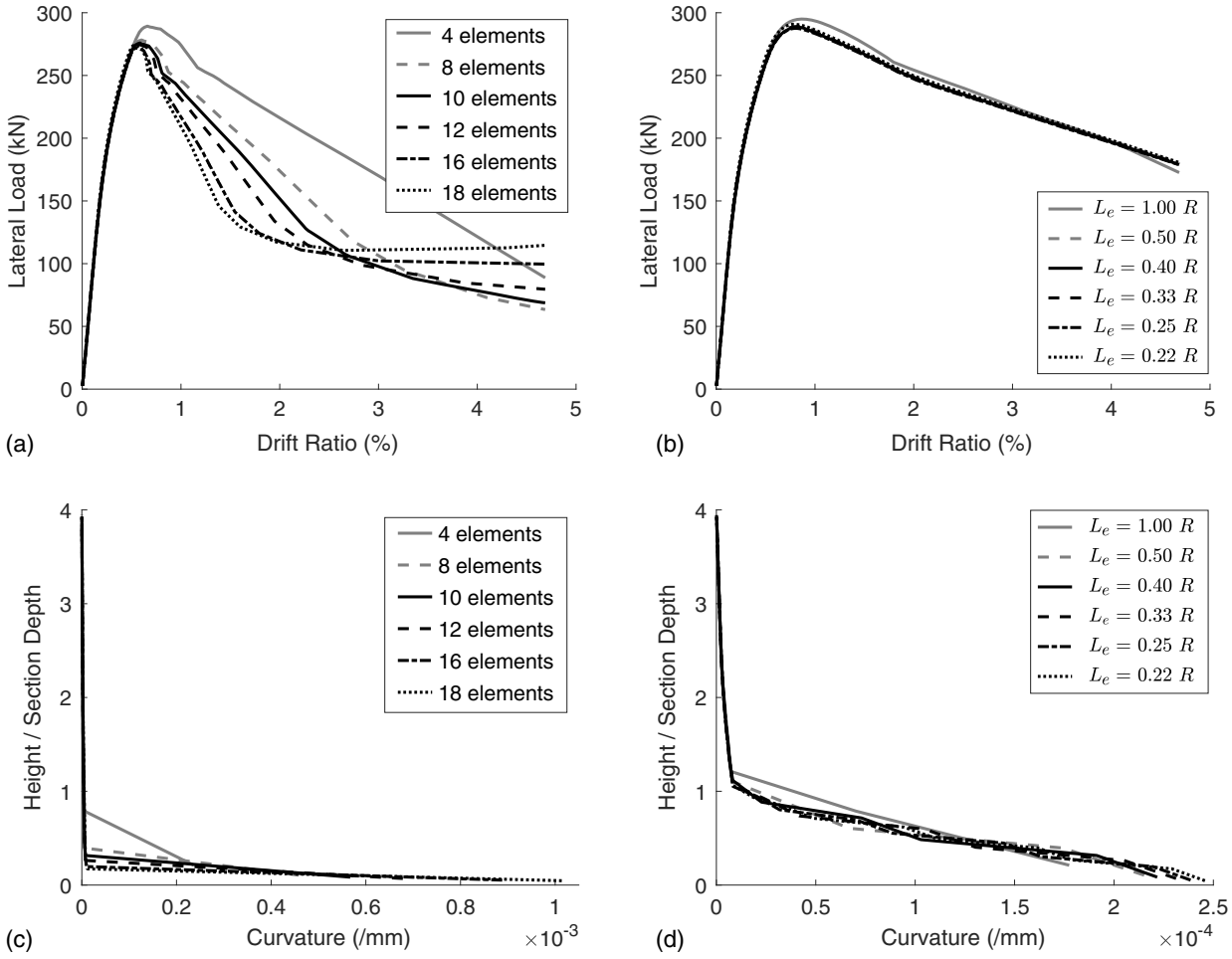

Fig. 7. Predicted response of specimen #17 in a pushover analysis using different mesh sizes: (a) lateral load versus drift ratio predicted by the local model; (b) lateral load versus drift ratio predicted by the nonlocal model; (c) curvature profile predicted by the local model; and (d) curvature profile predicted by the nonlocal model.

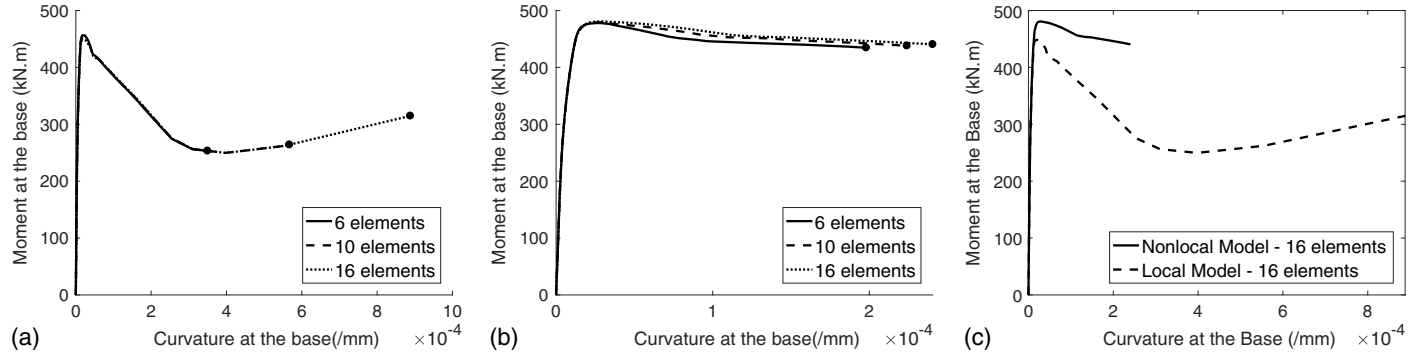

Fig. 8. Predicted moment versus curvature at the critical section (the cantilever base) of specimen #17 in a pushover analysis: (a) using different mesh sizes of the local model; (b) using different mesh sizes of the nonlocal model; and (c) using a mesh size of 16 elements for the local and nonlocal models.

critical section in the local simulation model. Once again, the figure highlights the convergence of the value of the maximum curvature predicted by the nonlocal model as the mesh is refined, whereas this value varies significantly for each mesh size in the local model (the difference between the maximum curvature predicted by a mesh size of 10 elements and 16 elements is about 7% for the nonlocal model and 37% for the local model). It is noted that because the Gauss Legendre integration rule is used, the location of the first integration point changes slightly as the mesh is refined; therefore, some minor differences in the maximum curvature values are to be expected.

- The nonlocal simulation model predicts a much shallower post-peak slope in the section moment-curvature response, as compared to the post-peak response predicted by the local model,

which is a direct consequence of enforcing the nonlocal interaction in the model. Another related consequence is that the predicted peak moment capacity of the section by the nonlocal model is higher than that of the local model. This difference is also reflected in the predicted peak force of the member in Fig. 7 (for specimen #17, the difference in the peak capacity between both models is about 6%). This result may be attributed to enforcing the nonlocality in the constitutive response of individual fibers rather than at the section level. In other words, the nonlocal interaction starts to take effect as individual fibers enter the softening regime, which is expected to occur prior to reaching the peak capacity of the section. This increase in the section capacity may be considered an artifact of the fiber-based nonlocal approach and could potentially be avoided in a nonlocal approach that enforces the nonlocality at the cross section level.

Mesh Sensitivity of the Local and Nonlocal Models Under Cyclic Loading

The member discretization was varied for both the local and nonlocal simulation models for six specimens (#4, #7 #8, #12, #15, and #18) to examine the sensitivity of the cyclic response of each specimen to the mesh size, and the predictions of both approaches were compared across the global and local response scales. Fig. 9 shows the predicted cyclic lateral load versus drift ratio using different mesh sizes for one representative column: specimen #18. Figs. 9(a–c) show the predictions of the local model using a mesh size of 6, 12, and 18 elements respectively, while Fig. 9(d) shows the predictions of the nonlocal DPC model using all different mesh sizes. In all subplots of Fig. 9, the observed response in the laboratory experiment is also displayed for reference. The subsequent figure, Fig. 10, shows the predicted curvature profile along the same specimen by both simulation approaches and for different mesh sizes. Qualitatively similar results were obtained for the other five specimens and were not included herein. Since the length of specimen #18 is 1,600 mm and the nonlocal scale for all specimens is equal to 400 mm, the mesh sizes of 6, 12, and 18 elements shown in Figs. 9 and 10 correspond to element size/ length scale ratios of 0.67, 0.33, and 0.22, respectively. Based on the figures, the following observations can be made:

- Figs. 9(a–c) reaffirm the sensitivity of the post-peak load-displacement response predicted by the local model to the mesh size, whereas a mesh-independent member response is predicted by the nonlocal model in Fig. 9(d). More pronounced mesh dependence throughout the entire loading history was particularly noted for specimens with relatively lower-axial load ratios η (for example, specimens #8 and #15). Generally, a lower-axial force on the column is associated with slower strength degradation in the cross section. This means that the concrete softening behavior contributes to the degradation in these specimens during most of the loading history. Conversely, the capacity of the concrete material in specimens subjected to larger axial

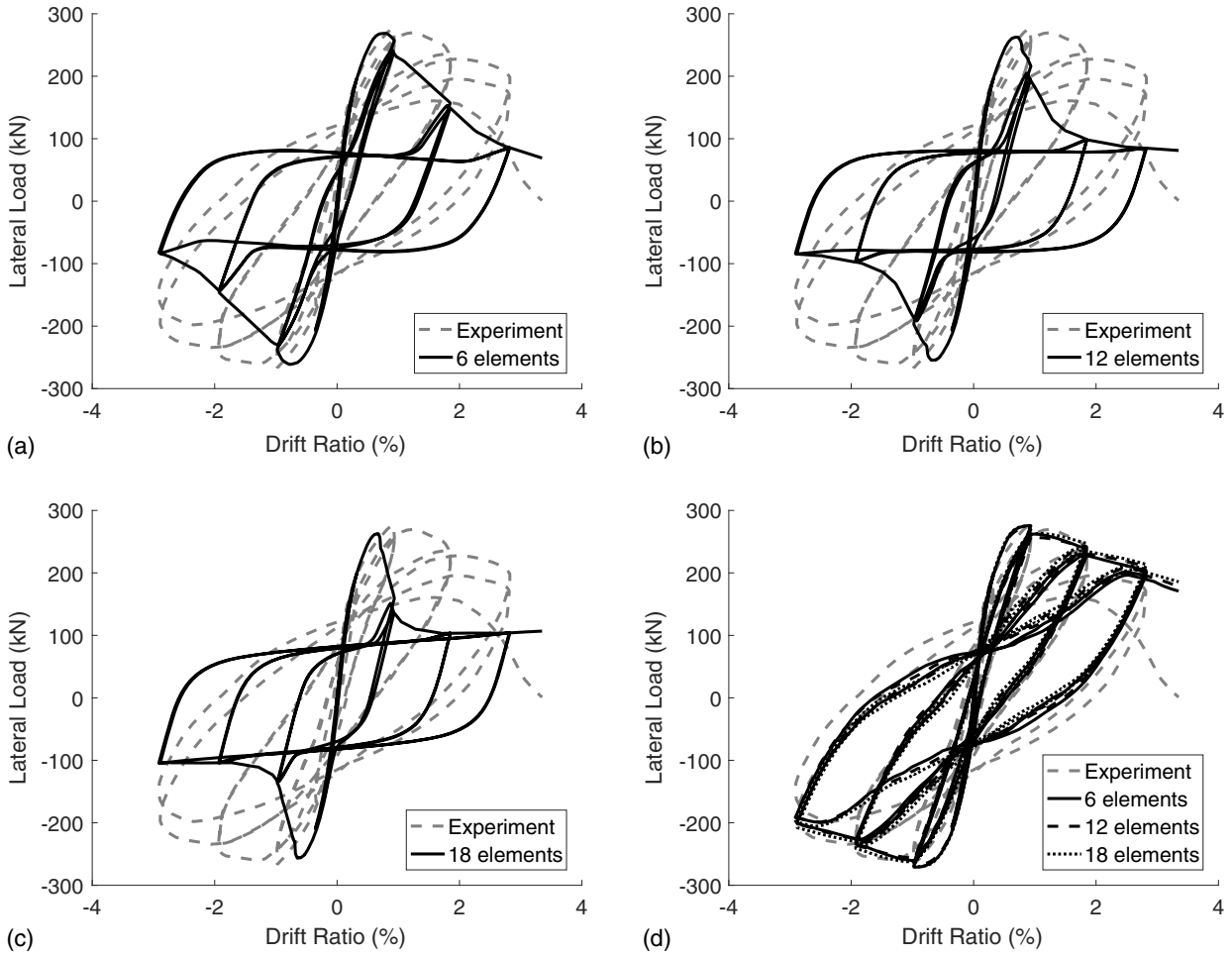

Fig. 9. Experimental observations and predictions of the load-displacement response of specimen #18 using different mesh sizes: (a) by the local model using 6 elements; (b) by the local model using 12 elements; (c) by the local model using 18 elements; and (d) by the nonlocal model.

J. Struct. Eng., 2020, 146(5): 04020052

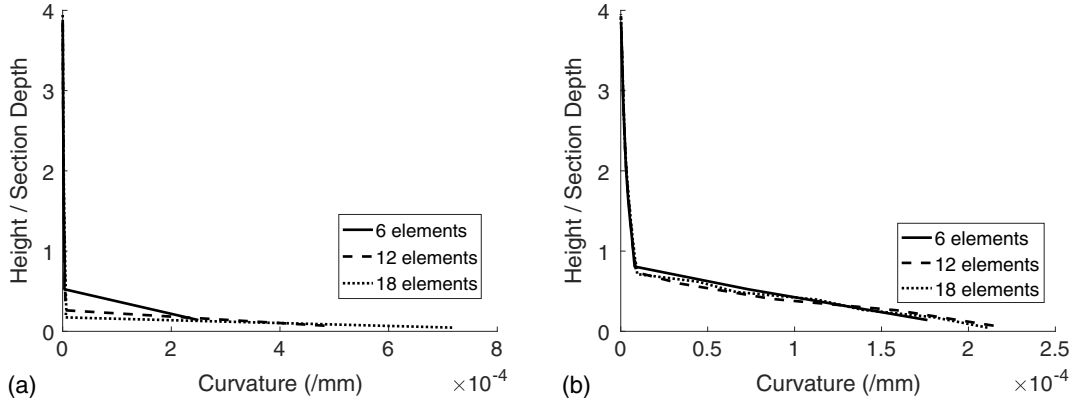

Fig. 10. Predicted curvature profile along specimen #18: (a) by the local model; and (b) by the nonlocal model.

loads diminishes rapidly (during the first few loading cycles). Beyond that point, the specimen response is primarily controlled by the hardening of the steel reinforcement and exhibits little sensitivity to the size of the mesh.

- The unloading and reloading stiffness and overall hysteresis loops predicted by the local and nonlocal models are qualitatively different. This result may be attributed to the nonphysical rapid degradation of the concrete capacity in the local model (caused by the mesh sensitivity of the response), such that the unloading-reloading behavior becomes artificially controlled by the steel material model (which does not incorporate any stiffness degradation). Comparing the predictions of the local model to the experimentally observed member response in Figs. 9(a–c) confirms this conclusion and reveals that key aspects of both the strength and stiffness degradation are not captured properly due to the mesh sensitivity of the underlying problem.
- The local simulation model fails to predict a unique curvature profile along the column, as shown in Fig. 10(a). Instead, the inelastic curvature appears to be localized to a single element at the column base, and the element size effectively acts as a length scale determining both the size of the plastic hinge zone and the value of the maximum curvature. However, the curvature profile predicted by the nonlocal model in Fig. 10(b) does not exhibit pathological mesh dependence and rapidly converges to a unique solution as the mesh is refined.

Validation Against Experimental Test Data

The nonlocal DPC model was used to blindly predict the strength and stiffness degradation of all 24 specimens presented in Table 1 under constant axial and cyclic lateral loading histories. The predictions of the nonlocal model were compared against the available load-displacement data for each specimen. Representative results are shown in Figs. 11 and 12, which display the predicted load-displacement response for ten specimens overlaid on top of the corresponding experimental observations. These results depict key aspects of the predicted response and the capabilities of the proposed constitutive model. Inspection of the nonlocal model predictions against the backdrop of the experimental observations reveals the following:

- As a general observation, the strength degradation trends of the RC columns examined in the current study are captured reasonably well by the proposed constitutive model, as seen in Figs. 9(d), 11, and 12. In some specimens, the predicted response exhibits qualitatively different post-peak behavior from the observed response [for instance, in Fig. 11(f), the model predicts in-cycle strength degradation in specimen #10 at a 3% drift ratio, which is not seen in the experiment]. This disagreement can be partially attributed to the error associated with estimating the softening slope of the core concrete in the column. To scrutinize the practical use of the proposed model as a blind prediction tool for RC members, it is combined with a rather simple and common method (the modified Kent–Park model) to determine this slope, without any parameter tuning to match the available experiments. As such, this choice results in the occasional under- or overestimation of the strength degradation of the member, as seen in Fig. 11(f). However, it is judged that the degradation trends predicted by the modified Kent–Park model are, overall, in reasonable agreement with the observed trends when used with the appropriate length scale parameter and combined with the proposed nonlocal material model.
- The predicted stiffness degradation during load reversal is generally in good agreement with the observed trends despite the fact that the stiffness degradation is assumed to progress in a relatively crude manner. In particular, the unloading-reloading stiffness is assumed to be constant within a single loading cycle (refer to Fig. 3) and informed by a single damage parameter. In some specimens [e.g., specimen #18 in Fig. 9(d) and specimen #12 in Fig. 11(b)], a somewhat pronounced pinching is detected in the predicted response, as compared to the observed response. This is not unexpected and may be explained by the simplifying assumptions imposed in the nonlocal DPC model. In particular, the concrete is assumed to possess zero tensile strength and a zero crack-closing modulus (i.e., the tensile cracks are assumed to be fully closed when load reversal from tension to compression occurs). The consequences of these assumptions are further discussed in the following subsection.
- Several of the specimens studied herein exhibit buckling and/or fracture of the longitudinal steel bars during the final loading cycles of the experiment. For example, rebar buckling and fracture accompanied by a significant loss in the load-carrying capacity were reported to occur in specimens #3, #4, #17 and #18 in the last one or two loading cycles. Consequently, substantial differences are noted between the predicted and observed responses for these specimens during the last few cycles. While simulating rebar buckling and fracture is outside the scope of this study, these mechanisms are observed to result in significant strength degradation, and incorporating them will be the focus of future studies by the authors.

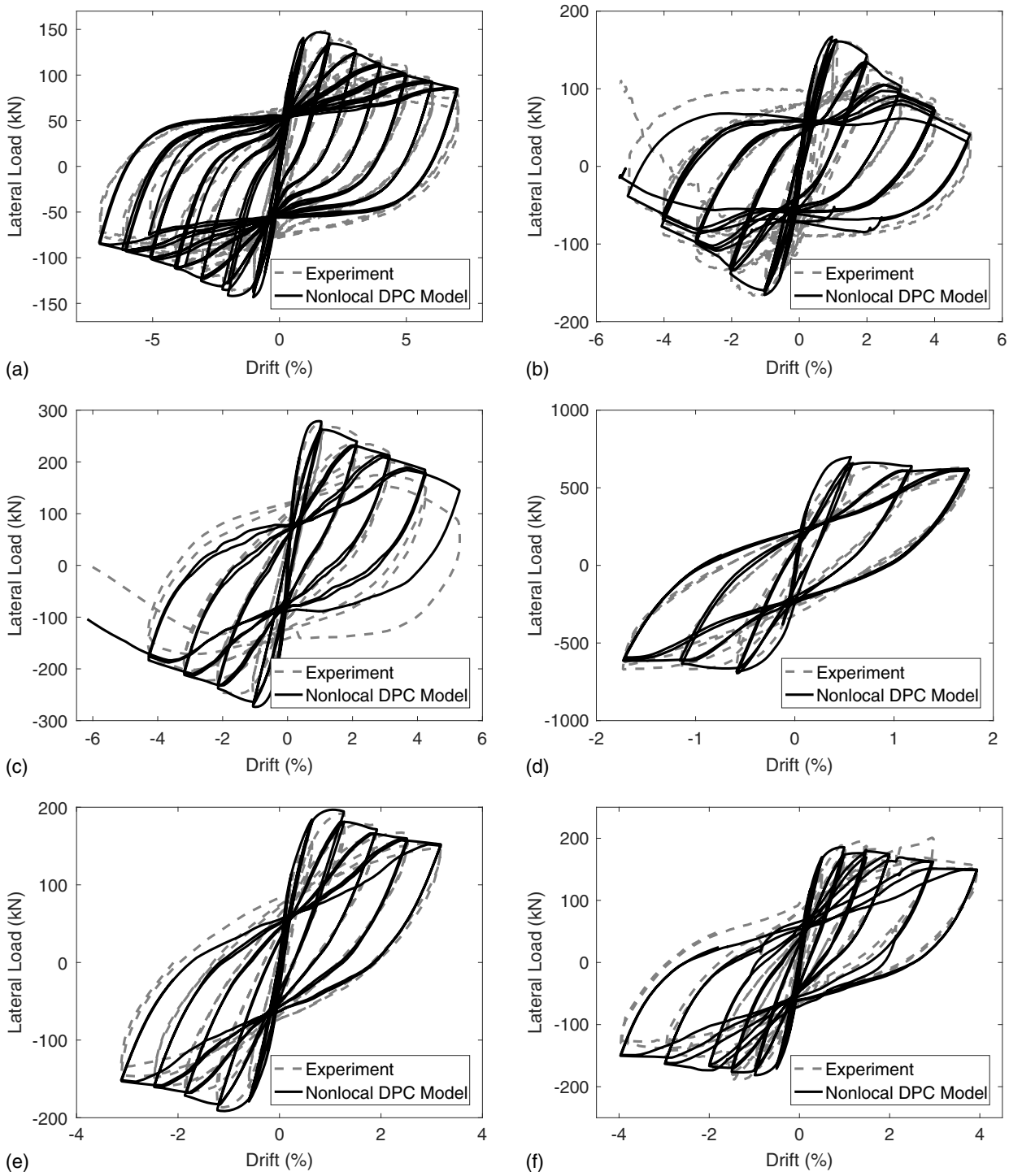

Fig. 11. Load-displacement response observed and predicted by the nonlocal DPC model for several RC columns: (a) specimen #13; (b) specimen #12; (c) specimen #17; (d) specimen #7; (e) specimen #1; and (f) specimen #10.

Effect of the Tensile Properties and Crack-Closing Mechanism

In the preceding subsection, the simulation models were created with suppressed tensile and crack-closing properties ($f_t = 0.0$ and $H_k = 0.0$) since no experimental data were available for calibrating these parameters for the considered specimens. In this part of the study, the sensitivity of the structural member capacity and deterioration to the tensile and crack-closing properties was studied for all 24 specimens. Figs. 13 and 14 show the load-displacement response predicted by the nonlocal models with and without incorporating the tensile capacity and tension-compression transition effects of the material for six selected specimens. The plots in Figs. 13(a, c, and e) and 14(a, c, and e) show the predicted response by the nonlocal DPC model, whereas the plots in Figs. 13(b, d, and f) and 14(b, d, and f) show the predictions of the nonlocal DPTC model.

The results in Figs. 13 and 14 reveal only minor differences between the member response quantities predicted with and without

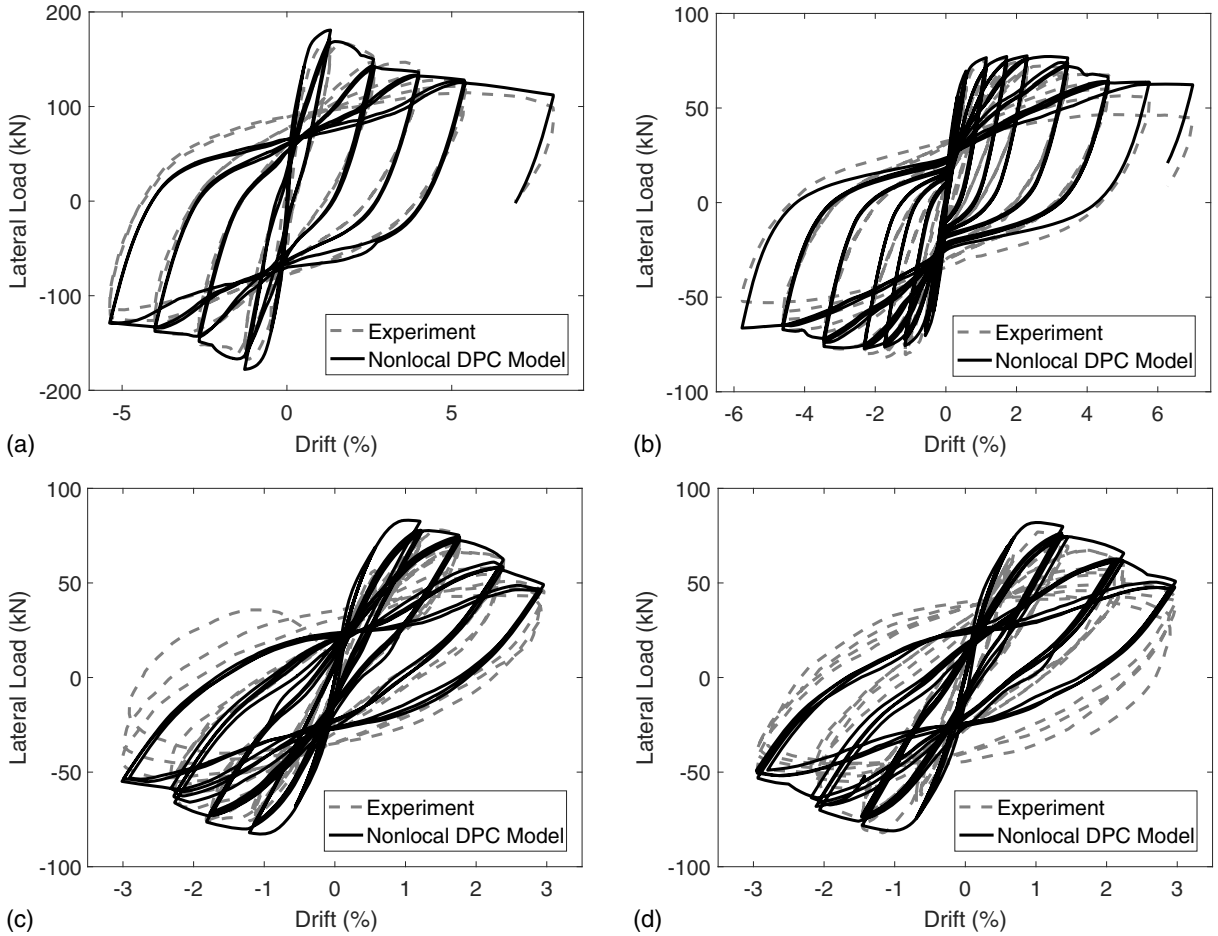

Fig. 12. Load-displacement response observed and predicted by the nonlocal DPC model for several RC columns: (a) specimen #20; (b) specimen #8; (c) specimen #4; and (d) specimen #3.

accounting for the tensile capacity of concrete; these differences are particularly seen in the early portion of the load-deformation response history (up to the peak capacity). It is noteworthy that the nonlocal DPTC model seems to overestimate the peak column capacity in many cases, as compared to the nonlocal DPC model and the corresponding experimental data. This trend may be attributed to several factors: (1) idealization of the base support in the numerical model as fixed may lead to overestimation of the column load-carrying capacity because it does not account for strain-penetration effects at the column base, (2) compressive strength of the confined concrete in the column may be overestimated by the confinement model, and (3) adopted tensile strength and degradation properties of the concrete, which are based on generally accepted values in the literature, may not accurately represent the observed properties in the experiments.

As expected, the agreement between the predicted and observed unloading and reloading stiffness in some specimens is improved by incorporating the crack-closing effects in the concrete material (and using the recommended value of $5\%E$ for the crack-closing modulus). This is the case, for example, for specimens #17 and #18 in Fig. 13 for which the hysteresis loops predicted by the DPTC model are in better agreement with the experimental observations than the response predicted by the DPC model. In other cases, the predicted unloading and reloading stiffness by both simulation models are almost identical. The results suggest that for the flexure-critical specimens examined in this study, neglecting the tensile capacity and precise crack-closure mechanisms may not significantly affect the predicted strength and stiffness degradation of the structural member.

Summary, Conclusions, and Future Work

A nonlocal methodology is presented to predict the deterioration of RC beam-columns subjected to a combination of axial and cyclic lateral loads using a FD displacement-based frame model. A nonlocal constitutive model and implementation procedure are proposed to simulate the behavior of concrete under uniaxial cyclic loading in a mesh-objective manner and extend the capability of a previously developed nonlocal framework to cyclic and seismic loading applications. The constitutive model is formulated in the combined framework of the theory of plasticity and damage mechanics. The model is capable of predicting the permanent deformations and strength and stiffness degradation of concrete under compressive and tensile loading, in addition to crack-closing effects during tension-compression transitions. The model incorporates a nonlocal formulation and an accompanying length scale parameter that enforce interactions between neighboring material points, thereby overcoming the mesh sensitivity associated with the presence of constitutive softening. The scope of the study includes the development, numerical implementation, and calibration of the nonlocal constitutive model, in addition to validation of its rigor and predictive capability against benchmark data. The performance of the nonlocal model is compared to the conventional modeling

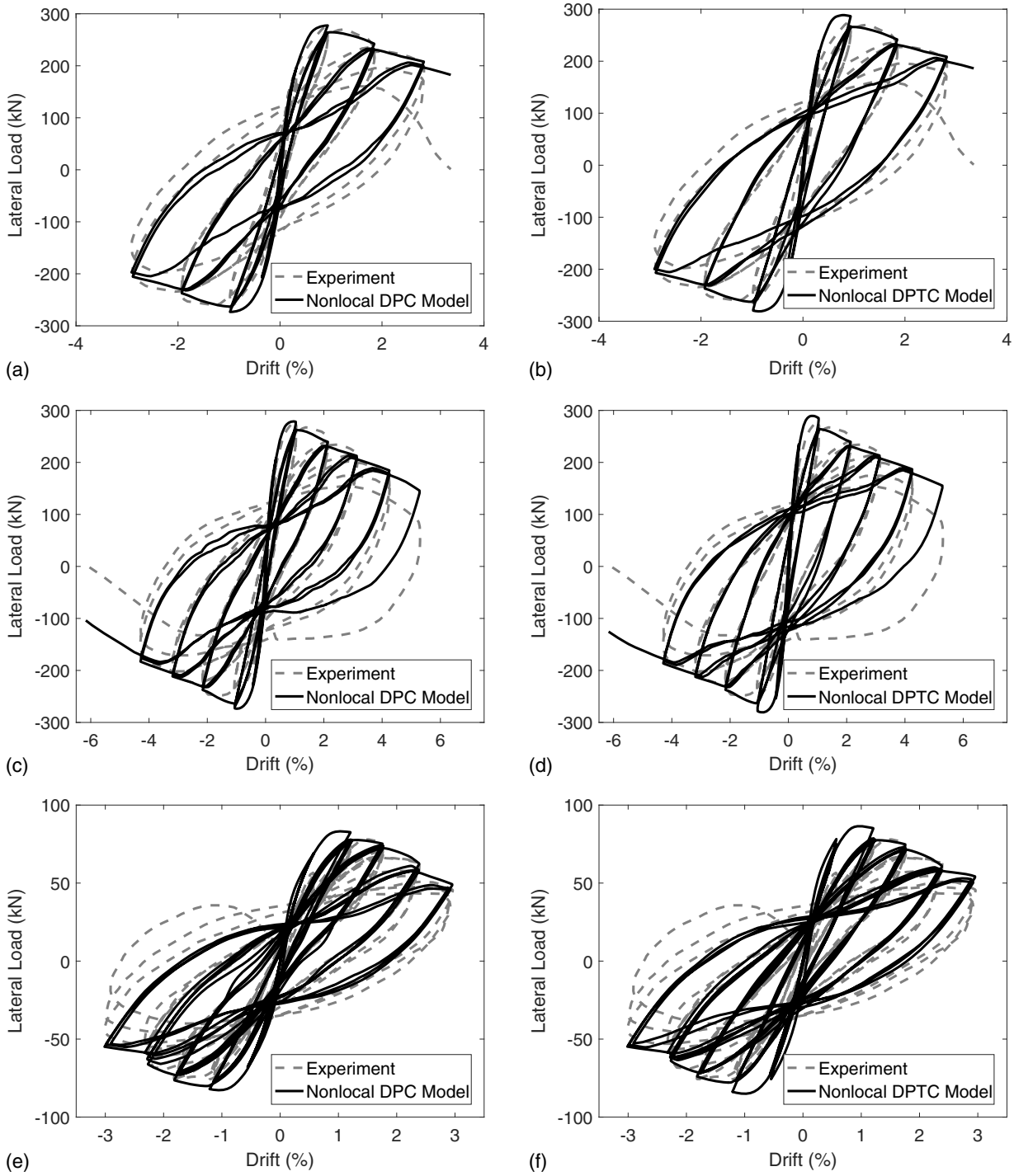

Fig. 13. Hysteretic load-displacement response of the following RC columns: (a) specimen #18 predicted by the DPC model; (b) specimen #18 predicted by the DPTC model; (c) specimen #17 predicted by the DPC model; (d) specimen #17 predicted by the DPTC model; (e) specimen #4 predicted by the DPC model; and (f) specimen #4 predicted by the DPTC model.

approach, and its predictive capability is demonstrated for 24 RC beam-columns subjected quasi-statically to reversed lateral loading cycles. The main findings of the study are summarized as follows:

- The proposed nonlocal methodology enables the prediction of RC component deterioration under cyclic lateral loading using FD displacement-based frame element models. The methodology retains the attractive features of FD models, including their ability to capture P-M interaction in structural members using uniaxial material-level calibrations and their ability to model the initiation and propagation of damage. The nonlocal methodology overcomes the weaknesses of FD models in the presence of material softening; these weaknesses include mesh dependence of the global member response and mesh-dependent localization of the inelastic deformation field.
- The mesh-objectivity of the response predicted by the proposed model is demonstrated via a parametric study on several RC columns subjected to monotonic and cyclic lateral displacements.

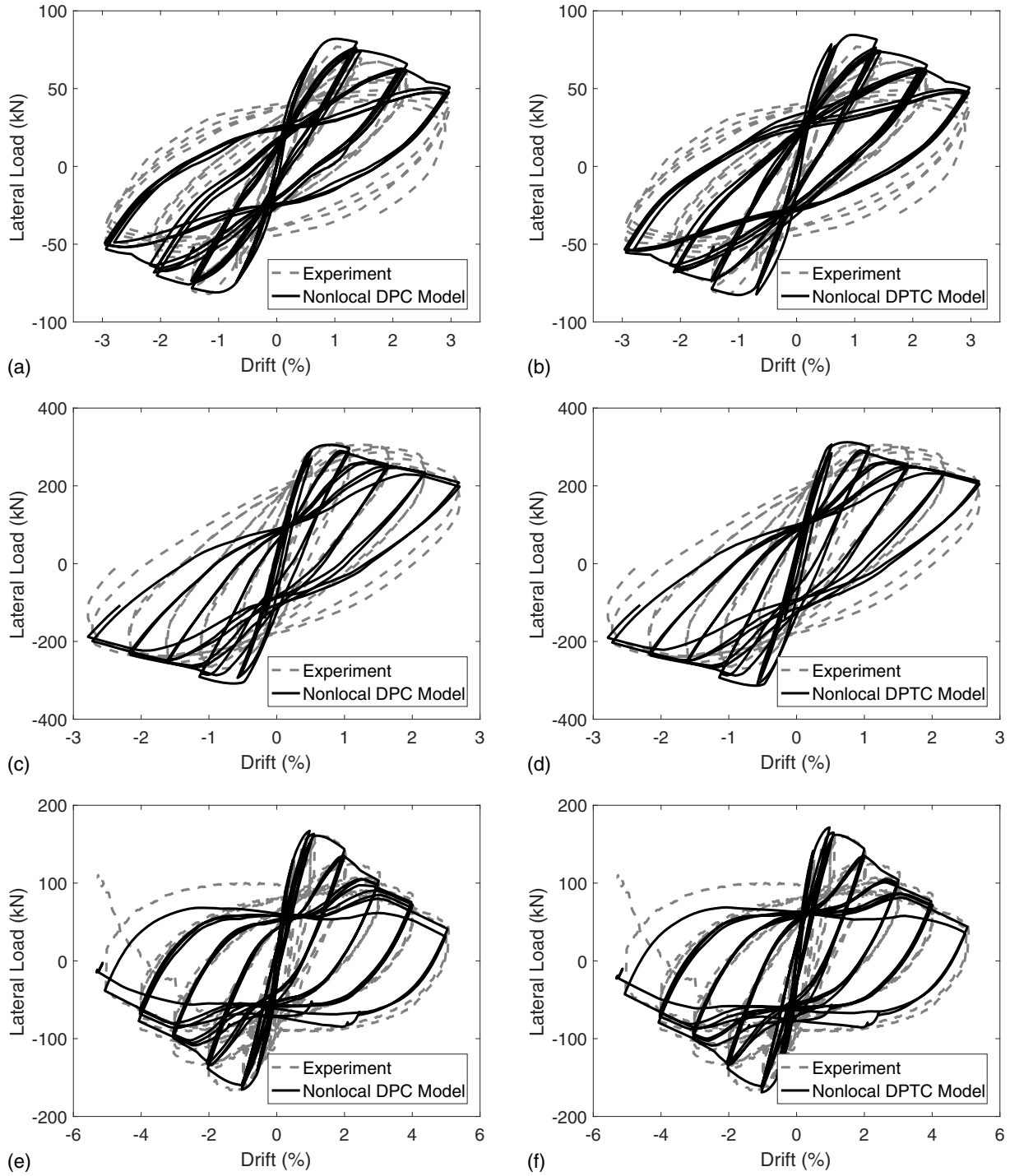

Fig. 14. Hysteretic load-displacement response of the following RC columns: (a) specimen #3 predicted by the DPC model; (b) specimen #3 predicted by the DPTC model; (c) specimen #23 predicted by the DPC model; (d) specimen #23 predicted by the DPTC model; (e) specimen #12 predicted by the DPC model; and (f) specimen #12 predicted by the DPTC model.

The proposed model successfully predicts a mesh-independent load-displacement response (which represents the global response of the member) and unique section curvatures (which represent the local response). The size of the plastic hinge zone in the column and the value of the maximum curvature are guided by the adopted nonlocal length scale.

- The proposed constitutive model appears to predict the response of concrete to uniaxial cyclic loading with good accuracy. Blind prediction of the load-displacement response of the column specimens considered in this study reveals that both the strength and stiffness degradation trends are captured reasonably well by the model. In its current form, the model is believed to provide an effective tool for predicting the hysteretic post-peak response of RC beam-columns due to concrete softening.
- The nonlocal interaction domain in the proposed model is interpreted as the length scale associated with the softening stress-strain relationship and can be directly obtained from experimental measurements on specimens of the appropriate size

or from common confinement models [e.g., the modified Kent–Park model (Scott et al. 1982)]. This approach was shown to achieve excellent agreement with the experimental tests considered in this study. In addition, mesh convergence studies demonstrate that this length scale does not impose stringent requirements on the mesh refinement of the analysis models.

- The proposed constitutive model retains the simple calibration and implementation procedure desired for uniaxial material models and particularly needed for seismic performance assessment applications. Most of the model parameters can be determined through conventional laboratory tests, and appropriate values and guidelines for determining the remaining parameters are provided; this includes the moduli controlling the stiffness degradation during load reversal, the crack-closing modulus, and the length scale that defines the range of interaction between neighboring material points.
- The proposed crack-closing model offers a novel approach to capturing the effects of tension-compression transitions on the behavior of concrete in a uniaxial context. Based on the results of this study, it is anticipated that incorporating the crack-closing mechanism may improve the agreement between the model predictions and experimental observations, particularly in the predicted unloading and reloading stiffness. However, this improvement may not be significant for flexure-critical RC columns. Incorporating such effects is recommended for applications where accurate simulation of the hysteretic tensile response of concrete is required. In such cases, further studies may be needed to more precisely calibrate the relevant model parameters.
- Determining the enhanced properties of the core concrete due to the confinement of the transverse steel reinforcement, particularly the softening slope, is one of the major sources of uncertainty associated with predicting the post-peak response of RC columns. In the proposed model, this slope informs the damage formulation and, therefore, directly affects the model predictions. While the careful selection of the appropriate confined concrete properties is generally advised, the modified Kent–Park confinement model used herein is deemed to provide satisfactory estimates for most specimens in the study.

A general limitation of the proposed framework is the inability to simulate other deterioration mechanisms in RC columns, namely, buckling and fracture of the steel reinforcing bars. The study demonstrates that these mechanisms may have a significant effect on the strength degradation of RC members and therefore must be incorporated in the simulation model or accounted for by other means. Future work will focus on simulating these phenomena in a fiber section construct using nonlocal uniaxial models for the steel material. The novel methodology recently developed by the authors to simulate buckling and fracture of one-dimensional steel bars (Kolwankar et al. 2017) will form the basis for further studies that incorporate the deterioration of steel rebar in RC member simulations.

Data Availability Statement

All data, models, and code generated and used during the study are available from the corresponding author by request.

Acknowledgments

This work was supported by the National Science Foundation (Grant No. CMMI 1434300), as well as graduate assistantships from the University of California at Davis. The findings and opinions presented in this paper are entirely those of the authors. The authors are thankful to Dr. Yannis Dafalias and Dr. Brian Giffin for their help with this development.

References

Addessi, D., and V. Ciampi. 2007. "A regularized force-based beam element with a damage–plastic section constitutive law." *Int. J. Numer. Methods Eng.* 70 (5): 610–629. https://doi.org/10.1002/nme.1911.

Ang, B. G., M. J. N. Priestley, and R. Park. 1981. "Ductility of reinforced concrete bridge piers under seismic loading." Ph.D. thesis, Dept. of Civil Engineering, Univ. of Canterbury.

Atalay, M. B., and J. Penzien. 1975. *The seismic behavior of critical regions of reinforced concrete components as influenced by moment, shear and axial force*. Technical Rep. Davis, CA: Earthquake Engineering Research Center, Univ. of California.

ATC (Applied Technology Council). 2009. *Quantification of building seismic performance factors*. Washington, DC: US Dept. of Homeland Security, FEMA.

Bažant, Z. P. 1976. "Instability, ductility, and size effect in strain-softening concrete." *J. Eng. Mech. Div.* 102 (2): 331–344.

Bažant, Z. P., and T. B. Belytschko. 1985. "Wave propagation in a strain-softening bar: Exact solution." *J. Eng. Mech.* 111 (3): 381–389. https://doi.org/10.1061/(ASCE)0733-9399(1985)111:3(381).

Bažant, Z. P., and M. Jirásek. 2002. "Nonlocal integral formulations of plasticity and damage: Survey of progress." *J. Eng. Mech.* 128 (11): 1119–1149. https://doi.org/10.1061/(ASCE)0733-9399(2002)128:11(1119).

Bažant, Z. P., and F. Lin. 1988. "Non-local yield limit degradation." *Int. J. Numer. Methods Eng.* 26 (8): 1805–1823. https://doi.org/10.1002/nme.1620260809.

Bažant, Z. P., and B. H. Oh. 1983. "Crack band theory for fracture of concrete." *Matériaux Constr.* 16 (3): 155–177. https://doi.org/10.1007/BF02486267.

Bažant, Z. P., and G. Pijaudier-Cabot. 1988. "Nonlocal continuum damage, localization instability and convergence." *J. Appl. Mech.* 55 (2): 287–293.

Bažant, Z. P., and G. Pijaudier-Cabot. 1989. "Measurement of characteristic length of nonlocal continuum." *J. Eng. Mech.* 115 (4): 755–767. https://doi.org/10.1061/%28ASCE%290733-9399%281989%29115%3A4%28755%29.

Berry, M., M. Parrish, and M. Eberhard. 2004. *PEER structural performance database users manual (version 1.0)*. Berkeley, CA: Pacific Earthquake Engineering Research Center, Univ. of California.

Brinkgreve, R. B. J. 1994. "Geomaterial models and numerical analysis of softening." Ph.D. thesis, Delft Univ. of Technology.

Chang, G., and J. B. Mander. 1994. *Seismic energy based fatigue damage analysis of bridge columns: Part 1—Evaluation of seismic capacity.* Alachua, FL: National Center for Construction Education and Research.

Coleman, J., and E. Spacone. 2001. "Localization issues in force-based frame elements." *J. Struct. Eng.* 127 (11): 1257–1265. https://doi.org/10.1061/(ASCE)0733-9445(2001)127:11(1257).

Feng, D., X. Ren, and J. Li. 2015. "Implicit gradient delocalization method for force-based frame element." *J. Struct. Eng.* 142 (2): 04015122. https://doi.org/10.1061/(ASCE)ST.1943-541X.0001397.

Gill, W. D., R. Park, and M. J. N. Priestley. 1979. "Ductility of rectangular reinforced concrete columns with axial load." M.S. thesis, Dept. of Civil Engineering, Univ. of Canterbury.

Grassl, P. 2009. "On a damage-plasticity approach to model concrete failure." *Proc. Inst. Civ. Eng. Eng. Comput. Mech.* 162 (4): 221–231.

Grassl, P., and M. Jirásek. 2006. "Plastic model with non-local damage applied to concrete." *Int. J. Numer. Anal. Methods Geomech.* 30 (1): 71–90. https://doi.org/10.1002/nag.479.

Ibarra, L. F., and H. Krawinkler. 2005. *Global collapse of frame structures under seismic excitations*. Berkeley, CA: Pacific Earthquake Engineering Research Center.

Jirásek, M. 1998. "Nonlocal models for damage and fracture: Comparison of approaches." *Int. J. Solids Struct.* 35 (31–32): 4133–4145.

Jirásek, M., and T. Zimmermann. 1998. "Rotating crack model with transition to scalar damage." *J. Eng. Mech.* 124 (3): 277–284. https://doi.org/10.1061/(ASCE)0733-9399(1998)124:3(277).

Kanda, M., N. Shirai, H. Adachi, and T. Sato. 1988. "Analytical study on elasto-plastic hysteretic behaviors of reinforced concrete members." *Trans. Jpn. Concr. Inst.* 10 (1): 257–264.

Karsan, I. D., and J. O. Jirsa. 1969. "Behavior of concrete under compressive loadings." *J. Struct. Div.* 95 (12): 2543–2564.

Kenawy, M., S. Kunnath, S. Kolwankar, and A. Kanvinde. 2018. "Fiber-based nonlocal formulation for simulating softening in reinforced concrete beam-columns." *J. Struct. Eng.* 144 (12): 04018217. https://doi.org/10.1061/(ASCE)ST.1943-541X.0002218.

Kolwankar, S., A. Kanvinde, M. Kenawy, and S. Kunnath. 2017. "Uniaxial nonlocal formulation for geometric nonlinearity–induced necking and buckling localization in a steel bar." *J. Struct. Eng.* 143 (9): 04017091. https://doi.org/10.1061/(ASCE)ST.1943-541X.0001827.

Kono, S., and F. Watanabe. 2000. "Damage evaluation of reinforced concrete columns under multiaxial cyclic loadings." In *Proc., 2nd US-Japan Workshop on Performance-Based Earthquake Engineering Methodology for Reinforced Concrete Building Structures*, 221–231. Berkeley, CA: Pacific Earthquake Engineering Research Center.

Légeron, F., P. Paultre, and J. Mazars. 2005. "Damage mechanics modeling of nonlinear seismic behavior of concrete structures." *J. Struct. Eng.* 131 (6): 946–955. https://doi.org/10.1061/(ASCE)0733-9445(2005)131:6(946).

Mander, J. B., M. J. Priestley, and R. Park. 1988. "Theoretical stress-strain model for confined concrete." *J. Struct. Eng.* 114 (8): 1804–1826. https://doi.org/10.1061/(ASCE)0733-9445(1988)114:8(1804).

Markeset, G., and A. Hillerborg. 1995. "Softening of concrete in compression-localization and size effects." *Cem. Concr. Res.* 25 (4): 702–708. https://doi.org/10.1016/0008-8846(95)00059-L.

Martínez-Rueda, J. E., and A. S. Elnashai. 1997. "Confined concrete model under cycling loading." *Mater. Struct.* 30 (3): 139–147. https://doi.org/10.1007/BF02486385.

McKenna, F., G. L. Fenves, and M. H. Scott. 2000. *Open system for earthquake engineering simulation*. Berkeley, CA: Univ. of California.

Menegotto, M., and P. Pinto. 1973. "Method of analysis for cyclically loaded reinforced concrete plane frames including changes in geometry and inelastic behavior of elements under combined normal force and bending." In *Proc., IABSE Symp. on Resistance and Ultimate Deformability of Structures Acted on by Well Defined Repeated Loads, Final Report*. Zürich, Switzerland: International Association for Bridge and Structural Engineering.

Okamoto, S., S. Shiomi, and K. Yamabe. 1976. "Earthquake resistance of prestressed concrete structures." In *Proc., Annual Architectural Institute of Japan (AIJ) Convention, Japan*, 1251–1252. Tokyo: Architectural Institute of Japan.

Palermo, D., and F. J. Vecchio. 2003. "Compression field modeling of reinforced concrete subjected to reversed loading: Formulation." *Struct. J.* 100 (5): 616–625.

Paulay, T., and M. N. Priestley. 1992. *Seismic design of reinforced concrete and masonry buildings*. New York: Wiley.

PEER (Pacific Earthquake Engineering Research Center). 2010. *Guidelines for performance-based seismic design of tall buildings*. Berkeley, CA: PEER, College of Engineering, Univ. of California.

Ramtani, S., Y. Berthaud, and J. Mazars. 1992. "Orthotropic behavior of concrete with directional aspects: Modelling and experiments." *Nucl. Eng. Des.* 133 (1): 97–111. https://doi.org/10.1016/0029-5493(92)90094-C.

Razvi, S., and M. Saatcioglu. 1999. "Confinement model for high-strength concrete." *J. Struct. Eng.* 125 (3): 281–289. https://doi.org/10.1061/(ASCE)0733-9445(1999)125:3(281).

Saatcioglu, M., and M. Grira. 1999. "Confinement of reinforced concrete columns with welded reinforced grids." *ACI Struct. J.* 96 (1): 29–39.

Salehi, M., and P. Sideris. 2017. "Refined gradient inelastic flexibility-based formulation for members subjected to arbitrary loading." *J. Eng. Mech.* 143 (9): 04017090. https://doi.org/10.1061/(ASCE)EM.1943-7889.0001288.

Salehi, M., and P. Sideris. 2018. "A finite-strain gradient-inelastic beam theory and a corresponding force-based frame element formulation." *Int. J. Numer. Methods Eng.* 116 (6): 380–411. https://doi.org/10.1002/nme.5929.

Saritas, A., and F. C. Filippou. 2009. "Numerical integration of a class of 3d plastic-damage concrete models and condensation of 3d stress–strain relations for use in beam finite elements." *Eng. Struct.* 31 (10): 2327–2336. https://doi.org/10.1016/j.engstruct.2009.05.005.

Scott, B. D., R. Park, and M. J. N. Priestley. 1982. "Stress-strain behavior of concrete confined by overlapping hoops at low and high strain rates." *ACI J.* 79 (1): 13–27.

Sheikh, S. A., and S. M. Uzumeri. 1982. "Analytical model for concrete confinement in tied columns." *J. Struct. Div.* 108 (12): 2703–2722.

Sima, J. F., P. Roca, and C. Molins. 2008. "Cyclic constitutive model for concrete." *Eng. Struct.* 30 (3): 695–706. https://doi.org/10.1016/j.engstruct.2007.05.005.

Sinha, B., K. H. Gerstle, and L. G. Tulin. 1964. "Stress-strain relations for concrete under cyclic loading." *ACI J. Proc.* 61 (2): 195–212.

Soesianawati, M. T., R. Park, and M. J. N. Priestley. 1986. "Limited ductility design of reinforced concrete columns." M.Eng. thesis, Dept. of Civil Engineering, Univ. of Canterbury.

Tanaka, H., and R. Park. 1990. "Effect of lateral confining reinforcement on the ductile behaviour of reinforced concrete columns." Ph.D. thesis, Dept. of Civil Engineering, Univ. of Canterbury.

Valipour, H. R., and S. J. Foster. 2009. "Nonlocal damage formulation for a flexibility-based frame element." *J. Struct. Eng.* 135 (10): 1213–1221. https://doi.org/10.1061/(ASCE)ST.1943-541X.0000054.

Watson, S., and R. Park. 1989. "Design of reinforced concrete frames of limited ductility." Ph.D. thesis, Dept. of Civil Engineering, Univ. of Canterbury.

Xenos, D., and P. Grassl. 2016. "Modelling the failure of reinforced concrete with nonlocal and crack band approaches using the damage-plasticity model cdpm2." *Finite Elem. Anal. Des.* 117 (Sep): 11–20. https://doi.org/10.1016/j.finel.2016.04.002.

Yassin, M. H. M. 1994. *Nonlinear analysis of prestressed concrete structures under monotonic and cyclic loads*. Berkeley, CA: Univ. of California.

Zahn, F. A., R. Park, and M. J. N. Priestley. 1985. "Design of reinforced concrete bridge columns for strength and ductility." Ph.D. thesis, Dept. of Civil Engineering, Univ. of Canterbury.

Zhang, G., and K. Khandelwal. 2016. "Modeling of nonlocal damage-plasticity in beams using isogeometric analysis." *Comput. Struct.* 165 (Mar): 76–95. https://doi.org/10.1016/j.compstruc.2015.12.006.